C00-2203-7

CRITICAL PHENOMENA IN THICK FILMS OF A BINARY LIQUID MIXTURE

by

Donald Thomas Jacobs

B.A., University of South Florida, 1971

M.A., University of South Florida, 1972

A thesis submitted to the Faculty of the Graduate School of the University of Colorado in partial fulfillment of the requirements for the degree of Doctor of Philosophy

Department of Physics and Astrophysics

1976

DISCLAIMER

This Thesis for the Doctor of Philosophy Degree by

Donald Thomas Jacobs

has been approved for the

Department of

Physics and Astrophysics

by

Richard C. Mockler

William J. O'Sullivan

Date December 3 1976

Jacobs, Donald Thomas (Ph.D., Physics)

Critical Phenomena in Thick Films of a Binary Liquid Mixture

Thesis directed by Professors R.C. Mockler and W.J. O'Sullivan

This work presents the first experimental data on the behavior of a critical system as it approaches two dimensionality. Measurements of the bulk coexistence curve using refractive index techniques are done on the binary fluid mixture methanol-cyclohexane. These measurements give the critical exponent $\beta = 0.326 \pm 0.003$ which agrees with recent Ising model calculations. This same binary fluid mixture was then constrained between two highly reflective, optically flat pieces of fused silica in an interferometer. The critical temperature and coexistence curve were determined as the spacing between the flats was varied from 1 μm to 60 μm. The critical temperature was directly measured for spacings between 3 and 60 μm. It was found that if the walls were close enough together ($\leq$ 6 μm) then the drops that form on phase separation would span the intervening space. The coexistence curves of these thick films ($\leq$ 6 μm) was determined from measurements of the difference in refractive index between the two phases that appeared as drops.

It was found that the shift in the critical temperature as the spacing was varied followed a logarithmic dependence. Such a dependence is not expected from Scaling Theory for an Ising model, but is to be expected of systems with effectively infinite range

interactions. The coexistence curves for each spacing of the thick film indicated that the critical exponent β was close to 0.5 which is the mean field (infinite range interaction) value and not the two-dimensional Ising model value of 0.125. The amplitude of the coexistence curves was found to vary with spacing as L^z with z in the range $0.6 \rightarrow 0.8$. This was a much larger dependence than expected from the theory. A comparison of the data and the theory and suggestions for new experiments are made.

This abstract is approved as to form and content. I recommend its publication.

Signed 
Richard C. Mockler

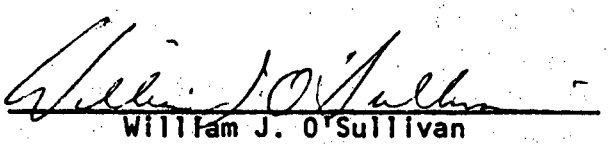
William J. O'Sullivan

ACKNOWLEDGMENTS

I must first thank my thesis advisors, Dick Mockler and Bill O'Sullivan. Without their support and persuasion this work would not have been possible. I have also enjoyed many helpful conversations with my fellow graduate students, particularly Charles Hartley, Bruce Ackerson, Chris Sorensen, and Benno Scheibner. Benno has also calibrated one of my thermistors for which I am grateful. Dan Anthony has helped me by constructing several pieces of electronic equipment and helping to set up, and take preliminary data on, the prism cell. I must also thank Bill Foote in Precision Shop and Spence Nye in Electronic Repairs for all of their help in keeping the equipment working. Chet Wells has instructed me on the ways of electronic wizardry and considerably expanded my knowledge in this area.

Finally, I must thank my wife, Donna, who suffered without complaining while I completed this degree. She supported me financially through the early years and has supported me emotionally throughout. For her sacrifices, in particular the typing of this thesis, I shall be eternally grateful. Had it not been for Donna and our daughter, Kathy, I would not enjoy the fruits of this labor.

TABLE OF CONTENTS

LIST OF TABLES

LIST OF FIGURES

CHAPTER I

INTRODUCTION

The study of critical phenomena has been ongoing for fifty or even a hundred years now (Stanley, 1971a). However, the main impetus has occurred since 1960 when Heller, Benedek and Jacrot, along with theoreticians such as Domb, Rushbrooke, Fisher and Marshall, realized that divergences in a variety of thermodynamic functions appear as powers of the deviation from criticality. These divergences are characterized by critical indices (the exponents in the power laws). The fascinating thing about these exponents is that they not only obey rigorous (via thermodynamics) inequalities (which for many are experimentally verified as equalities) but that they are the same for a wide variety of systems. Examples of systems exhibiting critical phenomena include superconductivity, liquid-gas, binary fluids, magnetic systems, growth of polymer chains, percolation (jumping from place to place on a lattice), well-developed turbulence and, to some extent, many particle interactions in high energy physics (Lubkin, 1972). It is for this reason that so much work has been done on critical phenomena in recent years. With such a variety of applications and with so much left to learn, it is indeed a very exciting field.

The background experiments and theoretical developments are rich and varied, and there are many reviews on the subject (Brout, 1965; Fisher, 1967; Heller, 1967; Kadanoff, 1967; Stanley, 1971a and 1971b; Levelt-Sengers, 1976) so I will refrain from expostulating on these, but let the interested reader refer to them. I will briefly discuss the nature of a critical point, and the definition of some of the critical exponents, but the details of some of the older phenomenological models will only be alluded to. A readable account of the above points is given by Stanley (1971a).

Universality and Scaling in Critical Phenomena

The concept that broad classes of systems can exhibit the same behavior near a critical point is called universality. This, along with the idea of scaling--that the behavior near the critical point is unchanged as the scale of length (and other variables) is changed--were realized in 1966 when Kadanoff proposed that, near a critical point, if the length scale is changed the effective Hamiltonian should remain invariant. Using this, he was able to recover the scaling laws of Widom and others, and also to obtain relations among the critical exponents. Kenneth Wilson, in 1971, was able to show exactly how this is done and to provide a method ("Renormalization Group") for approximating the critical exponents for the various models. The Renormalization Group approach is discussed in Appendix A.

It is important to take a moment to realize the nature of this method that uses the invariance of the Hamiltonian to change

of scale (scale symmetry). (The invariance of the Hamiltonian to a set of transformations changing the scale implies the set of transformations forms a group, the change of scale, or length, and is called "renormalization", hence, "Renormalization Group". This is to be distinguished from the field theory concept, where renormalization involves divergences and cut off parameters--this distinction will be made clearer later.) Scale symmetry is a "space-time" symmetry, others of which lead to conservation of energy and momentum, instead of an "internal" symmetry, which leads to conservation of various "quantum numbers". The advantage of working with such a symmetry is obvious, as the nuclear and particle physicists can testify. There are advantages to investigating exact and approximate symmetries. By utilizing the approximate scale symmetry, one can recover the relations among the critical exponents (i.e., equalities which are experimentally verified), the scaling laws of Widom, and universality.

It is possible to separate any physical problem into a model and the geometry where the model is used. The geometry can be described independently of the model by the symmetry it possesses. For instance, the harmonic oscillator is a model but the harmonic oscillator problem can not be solved until the geometry is provided; however, the geometry can be studied in general and then combined with various models to obtain values of physically interesting quantities. The result of applying group theory to a problem is that only relations between quantities can be found but not the values of the quantities (unless a model is employed). The significance of the Renormalization Group approach is that it

provides an approximate description of the geometry on which the many models currently in existence can be used.

The so-called "Scaling Theory" is a consequence of the Renormalization Group approach and thus can provide realtionships between critical exponents. It is very important to remember that many approximations are involved in the Renormalization Group approach so that the predictions of Scaling Theory are just that--predictions. The work described in this thesis is the first experimental test of some of these predictions. The results of the Renormalization Group procedure have thus far agreed with experimental results.

Qualitative Features of Critical Phenomena

Before jumping into the details of this paper, it is useful to consider a simple physical picture of what occurs at a critical point. First, consider a liquid-gas transition; we realize that there is increasing interaction among the molecules as the critical temperature is approached from above as evidenced by the deviation from the ideal gas law. In fact, by utilizing the Van der Waals equation of state for real gases (a "mean field" model), one can exhibit a critical point and critical exponents (which are all at variance with experimental values on bulk systems).

Now we consider the Ising model of magnetic systems (which corresponds to the lattice-gas model for liquid-gas systems) where one imagines a spin to be pointing up or down on each lattice site. For liquid-gas systems, the volume is partitioned to microscopic cells allowing only one molecule on each site (finite size of the

particles) where spin up corresponds to a molecule being present and spin down corresponds to no molecule on the site. However, the molecules are not constrained to a site. For the temperature, T, much larger than the critical temperature, T_c, we see random flipping of the spins, corresponding to freely moving gas molecules. As $T \to T_c^+$ small domains of correlated spins occur as the spin-spin interaction becomes important, and their size increases as $T - T_c \to 0$. (For the fluids, droplets begin to form, increasing in size as $T - T_c \to 0$.) When the average size of the droplets becomes the same order of magnitude as the wave length of visible light, light is strongly scattered (called critical opalescence) giving vivid experimental justification of the idea that near the critical point the correlation length, ξ, becomes very large. At the critical point the long range order (droplets) characteristic of the region $T > T_c$ gives rise to a liquid (or fluid) phase or of magnetic domains characteristic of $T < T_c$.

To be more specific, let us consider the Ising model (since we will use it shortly), which is a d-dimensional lattice and on every lattice site, $\vec{n}$, a spin is situated. The Ising Hamiltonian is (without the factor, $(kT)^{-1}$, included)

$$H_I = -H' \cdot \sum_{\vec{n}} S_{\vec{n}} - K \sum_{\vec{n},\vec{\tau}} S_{\vec{n}} \cdot S_{\vec{n}+\vec{\tau}}$$

where $S_{\vec{n}}$ stands for the spin on site $\vec{n}$ which can point up or down ($S_{\vec{n}} = \pm 1$); the summation goes over all sites $\vec{n}$; $\vec{\tau}$ are the unit vectors in the lattice which shift from a site to its nearest neighbor's. The external magnetic field is H', and K is the

spin-nearest neighbor spin coupling constant. (For a liquid-gas (lattice-gas model) $S_{\vec{n}} = 2(\rho_{\vec{n}} - \frac{1}{2})$ where $\rho_{\vec{n}} = 1$ if there is a particle and 0 if no particle on site $\vec{n}$; K gives the strength of the attractive force among the particles, and the external field, H', is interpreted as the chemical potential, μ, times the number of particles: $H' = \mu N$.) The procedure is to calculate the partition function, Z, and so the free energy density, F (allowing all the other thermodynamic quantities to be calculated), from the Hamiltonian

$$Z = < e^{-\beta H} >, \qquad F = -\ell n(Z)/V$$

where < > denotes the sum over all possible states of the system. This can be done exactly for d = 1 and 2, but only approximately for d = 3. The problem with the approximations done for d = 3 are that they assume large T so $(kT)^{-1}$ is small and they expand in $(kT)^{-1}$ assuming a small correlation length, ξ. However, as criticality is approached, $\xi \to \infty$ and the approximations of some thermodynamic functions develop singularities at $T = T_c$. There is a procedure to correct this (Padé approximates), but the problem can be circumvented by using the Renormalization Group approach.

The correlation length, ξ, which becomes very large close to the critical temperature, T_c, but assumes some mean molecular size, ξ_o, well away from the critical point, can be written as a power law divergence: $\xi = \xi_o[(T - T_c)/T_c]^{-\nu}$ where ν is a critical exponent that is independent of the details of the system but depends on general features such as boundary conditions and dimensionality. Other critical exponents can be defined by the power

law divergences of various thermodynamic quantities. Some of the exponents with their definitions and values are shown in Table I.

Considerable theoretical interest has been shown in the behavior of critical systems in a dimensionality other than three. This is partially due to the solutions to the models being easier (an exact solution can be obtained for the two-dimensional Ising model (see McCoy and Wu, 1973)) but also because the Renormalization Group Theory allows the critical exponents to be approximated in a continuous fashion knowing the dimensionality and model (see Appendix A). "Scaling Theory" describes the crossover from three- to two-dimensional behavior as one of the system's dimensions becomes small near the critical point. Since the correlation length, ξ (see Table I), becomes quite large near T_c then L, the size of the system in one of its dimensions, can be smaller than ξ. Then the system is constrained from having fluctuations of size ξ in one dimension and so may approximate a two-dimensional system. (This theory is presented in Chapter 4.)

The dimensionality of real films can be divided into three main categories (Fisher, 1973) depending on the relative size of the average molecular (or lattice) size, ξ_o, the range of interaction, ξ, and the film thickness, L. First, purely two-dimensional films can be divided into very thin films ($L << \xi_o \sim \xi$) (which can be realized in superconductors and where a classical or mean field description applies) and thin films ($L \sim \xi_o$) which includes monomolecular and bimolecular films. Second, thick films ($L >> \xi_o$) which are expected to exhibit "crossover" from three to two dimensions as the critical point is approached. And last, bulk

TABLE I

DEFINITIONS AND VALUES OF SOME CRITICAL EXPONENTS

Exponent	Definition	Model Values			Experimental Values	
		Ising		Mean Field		
		d = 2	d = 3		d = 2	d = 3
α	$C_v \sim \lvert\varepsilon\rvert^{-\alpha}$	0(log)	$\sim$ 1/16	0	?	?($\sim$ 0.1)
β	$\Delta\phi \sim \varepsilon^{\beta}$	1/8	$\sim$ 5/16	1/2	?	$\sim$ 0.34
ν	$\xi \sim \varepsilon^{-\nu}$	1	$\sim$ 0.64	1/2	?	$\sim$ 0.64
η	$g(r) \simeq \frac{Ae^{-r/\xi}}{r^{1+\eta}}$	1/4	$\sim$ 0.04	0	?	?($<$ 0.1)

films ($L > 10^6 \xi_o$) where three-dimensional behavior is expected to predominate. For our binary fluid system, $\xi_o \sim 3$ Å, so that a "thick" film is one which varies from $\sim$ 100 Å to $\sim$ 300 μm in one of its dimensions. A bulk fluid has each dimension larger than $\sim$ 300 μm.

Statement of the Problem

This work was undertaken to experimentally determine the behavior of a binary fluid system near its critical point for thick films that may simulate a two-dimensional system. Recent predictions have been made on the behavior of the critical temperature and the power law divergences of thermodynamic quantities near the critical point as a function of the film thickness. These predictions are tested by the work described here.

CHAPTER II

EXPERIMENTAL BACKGROUND AND APPARATUS

Experimental Background

In spite of theoretical predictions that changes would be seen in the critical exponents and temperature as a function of dimensionality, very little work has been done to test these predictions. A few measurements have been done on the critical temperature of helium films (Brewer, 1970; Guyon, 1973) but, as discussed in Appendix A, they are in a different universality class than Ising-type systems which include binary fluid mixtures. Some superconductivity work (Guyon, 1973) has also been done but again, they are not Ising systems. Recently, data on Ni films near the Curie point have shown an $L^{-\lambda}$ dependence but the data are not conclusive (Lutz, et.al., 1974). Therefore, it was decided that a look at the properties of thick films for an Ising class system was needed.

First, binary fluids are shown to be consistent with the universality class ($n = 1$) of the Ising (lattice-gas) class, which, as discussed in Appendix A, also includes simple fluids and some magnetic systems. In order to do this, the measurement of a critical exponent for a binary bulk fluid mixture was shown to agree with the Ising model predictions and measurements on simple fluids. This is not to say that this was the first measurement of

the coexistence curve for a binary fluid, but, as will be shown, the method used allowed a much more accurate determination of the curve.

Therefore, the first experiment was the measurement of the critical exponent, β, which determines the shape of the coexistence curve, and is an exponent that can be measured quite precisely. For binary fluid mixtures, a variety of choices exist for the order parameter (e.g., concentration in mole fraction, volume fraction, weight percent, etc.) but since the volume fraction seems to give the most symmetric coexistence curve experimentally (Greer, 1976), it was chosen as the order parameter in this experiment. The simple Ising model predicts a completely symmetric coexistence curve.

To measure the coexistence curve, the change in the volume fraction between the two phases was determined by employing refractive index techniques. The coexistence curve, of course, can be determined in several ways. One way would be to prepare a set of vials of various compositions and measure the height of the meniscus as a function of temperature. Another would be to observe the temperature at which the meniscus "disappeared" for different compositions. However, these are not very precise methods for several reasons. First, it is difficult to prepare the exact composition desired, particularly if the sample volume is small. Second, the meniscus, which gets broad close to T_c but laps up on the glass far from T_c, cannot be accurately located. Third, the temperature at which the meniscus disappears cannot be accurately measured. Another problem arises in making sure that the same

level of impurities is present in all the samples, since even minor impurities can cause very large changes in the critical temperature, and so ruin any intercomparison of data between samples.

A second and much better method of determining the coexistence curve is to simultaneously measure the density of the upper and lower phase for various temperatures. We chose one precise method of measuring the density, namely, the refractive index. The bulk refractive index of our volatile fluid mixture was measured, since it allows the critical exponent, β, to be determined, as well as checking for any anomalies in the rectilinear diameter. To measure the bulk refractive indices of our fluids a prism cell was used since it allowed the fluids to be sealed and also since a good quality spectrometer was available. From the measured index of refraction in the upper and lower phases, the change in volume fraction could be calculated, so that the critical exponent, β, (the critical exponents were defined in the first section of this work) could be determined and compared with values measured for different systems that were also considered to be Ising-like. Since refractive index techniques were to be used in thick films, it was necessary to be sure there were no serious errors in using the Lorentz-Lorenz relation. Thus, the refractive index anomaly was remeasured using the critical concentration of the fluids (which was determined from the coexistence curve). Also, the density anomaly near the critical point was checked by Scheibner (1976) to determine the size of this effect, although it was not expected to be very large based on other measurements on similar

systems. The relative importance of the refractive index and density anomalies was determined near the critical point.

After these preliminary investigations, a fluid sample was captured between two optical flats and squeezed down to a thick film whose thickness could be varied in order to determine the critical temperature and exponent dependence. The Ising-like system chosen was a binary fluid mixture simply because it has several advantages for the experimentalist. First, the pressure need not be controlled due to the effectively infinite compressibility of liquids. (Since our cells are sealed at room temperature then the pressure increase in raising the cell temperature 25 K causes the critical temperature to increase by $\sim$ 10 mK. (Washburn, 1928).) Second, for the same reason, gravity effects are typically much less for a binary fluid mixture than they are for a simple liquid-gas transition. And, third, the critical temperature is experimentally very easily accessible--typically 10 K to 40 K above room temperature--so temperature control is greatly simplified. There are other advantages which will be pointed out later.

The binary fluid mixture chosen was one that had a large refractive index difference but a small density difference between the two components (so that the gravity effects were very small) and one for which the critical temperature and concentration were fairly well known. These are all fairly severe restrictions, especially the restriction that the density difference be small while the refractive index difference is large. The best choice that we could find was the system methanol-cyclohexane. It was also the system that Hartley (1974) had used in measuring the

preliminary data on the refractive index anomaly. We wished to use this data, as well.

Experimental Apparatus

Prism Cell

It was first necessary to construct a cell with which to measure the refractive index of the two phases and obtain the coexistence curve, and with it, the critical exponent, β, which would indicate the universality class to which that binary mixture belongs. A convenient and reasonably accurate way to measure the absolute bulk refractive index of volatile fluids, which must be sealed to prevent impurities or evaporation from occurring, was to use a prism cell as a simple, efficient and accurate method. The prism cell that we designed, as shown in Figure 1, was a piece of aluminum carefully shaped to be an equilateral triangle. The cell was anodized in order to prevent reaction with the fluids which were contained in a one-inch hole bored parallel to the base. The fluids were captured by two optically flat ($\lambda/20$) pieces of glass and sealed with teflon. The cell was heated by means of three heaters located symmetrically inside it and the temperature was monitored by a thermistor. The pertinent measurements which needed to be taken with this cell were the prism angle (the angle between the two windows), the undeviated angle through the refractometer and the deviated angle through the fluid. This "general physics" piece of equipment provided very precise measurements. The geometry is shown in Figure 2. A laser was used as a

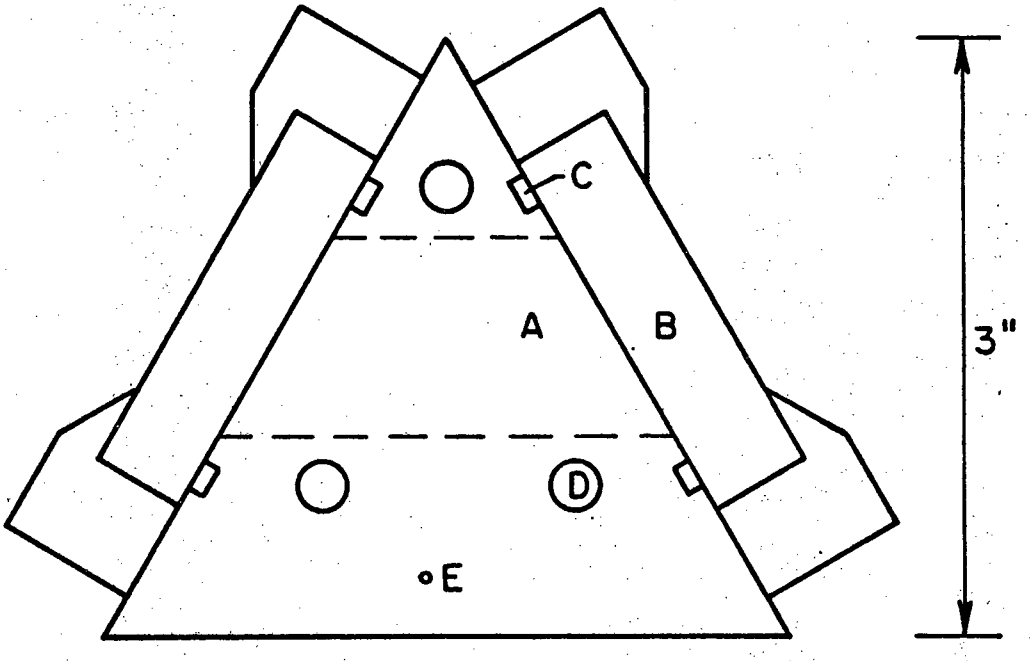

Figure 1: The prism cell used in this experiment is made of anodized aluminum with a one-inch bore (A) for the fluids which are captured by two optically flat pieces of glass (B) and sealed with teflon (C). The cell is heated by three symmetric internal heaters (D) and the temperature is monitored with a thermistor (E).

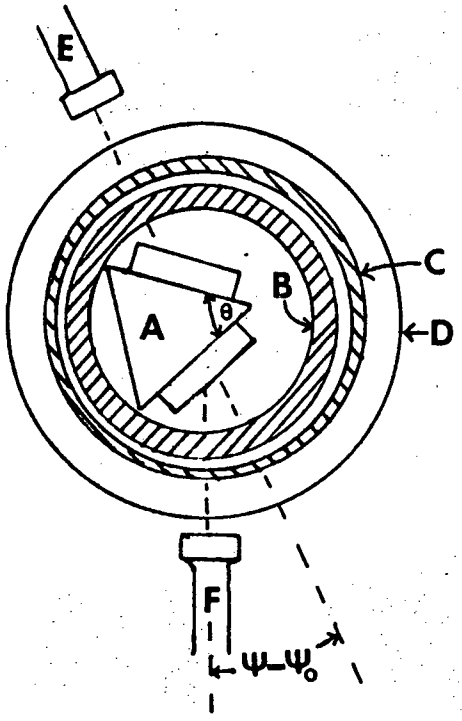

Figure 2: Prism Cell Geometry. The prism cell, A, is placed inside a heat shield, B, which is in turn inside a vacuum envelope, C. The system is placed on the spectrometer, D, so that the light from the collimator, E, will be deviated through an angle $\psi - \psi_0$ into the telescope, F.

monochromatic source with a rotating ground glass screen "mixing the modes" and so eliminating the annoying "speckles".

Variable Spacing Cell

The next step was to devise a means by which some of the anomalous refractive index data above the critical temperature could be retaken while also using the same cell to capture a thick film of fluid. It was necessary that the spacing be variable and directly measurable while allowing the behavior of the fluid to be determined. Toward this end we decided to use a differential refractometer that was a modified version of what Hartley had used in his anomalous refractive index measurement.

We again took two optically flat ($\lambda/100$) pieces of quartz that were coated with very high reflectance coatings, 99.0% at 6328 Å (He-Ne laser line). The high reflectance coatings allowed a very sharp and distinct fringe to be seen, which was ideal for both the refractive index measurements and also for observing the behavior of the fluid between the flats. The cell was modified from the design of the cell that Hartley had used to that shown in Figure 3. The two flat pieces of quartz, which we will also refer to as mirrors or simply "flats", were each sealed in one half of the cell. The two halves of the cell were then connected by means of a stainless steel bellows, which allowed a reservoir of fluid to surround the sample of fluid that was under study between the flats, and also allowed the spacing between the flats to be continuously varied by means of the differential screws which were located at the perimeter of the cell. The three differential

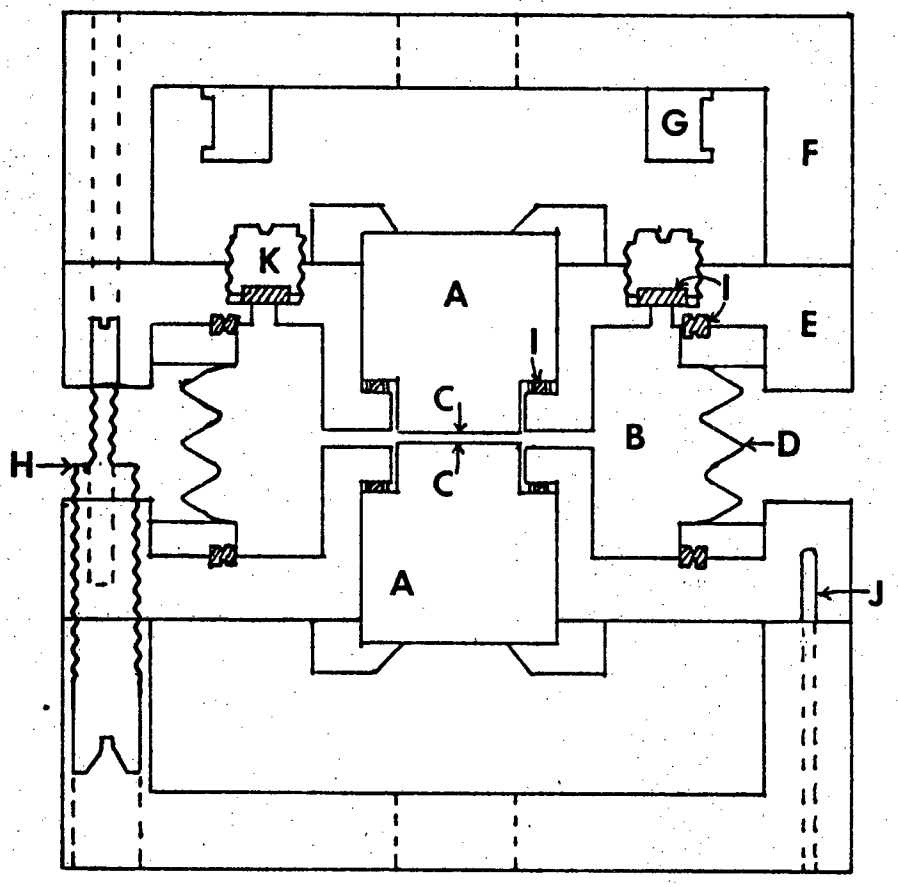

Figure 3: Variable spacing cell with A - the quartz (fused silica) flats, B - the fluid cavity, C - the high reflectance coating, D - the stainless steel bellows, E - the stainless steel cell half, F - an aluminum cell cap containing a heater form, G, H - an invar differential screw, I - a teflon seal and J - a thermistor well.

screws had fifty-two and fifty-one threads per inch on the outside and inside respectively, which allowed very fine control of the spacing. Of course, it also necessitated great care in setting up the original spacing because, with the approximately one inch of differential screw, the mirrors can only move about 240 μm. The cell halves were also made out of stainless steel and the seals were teflon (except in the refractive index measurements, where indium seals were used on a similar cell--the difference between the cells was very slight and the distinction will be made where appropriate.) The cell had two end caps which contained the heater coils. This allowed the heater to be removed when cleaning, filling and massing the cell and also allowed the radiated heat from the heater to be contained within the cell. The heater coils were matched in resistance to ± 0.1 Ω. Between the two cell halves were three turns of one-and-one-half inch braid to provide better thermal conduction between the cell halves. The cell was thermally isolated from the outside environment by being placed on nylon posts inside a half-inch thick aluminum heat shield which was then attached to a surrounding vacuum envelope by an additional set of nylon posts. This assured very little conduction loss between the pieces and almost all radiation exchange, thereby providing uniform heat loss and small temperature gradients across the cell. Of course, with the nylon posts supporting the cell, there was some extra heat loss down through the nylon supports which was compensated for by a trim pot attached externally to the heater coil remote from the nylon supports. Thus, just the amount of power that was lost through the nylon supports could be subtracted from

the other side of the cell. We describe later, in more detail, the procedure used to balance the power losses. The cell was filled by means of the fill-hole plug, taking approximately 50 ml of fluid, while still allowing a small air space. (See Figure 4.)

Refractive index techniques were used to determine the fluid's behavior since, as the refractive index of the fluid changes, the optical path length will change causing the observed fringe to shift. Since the fringes are so very narrow, the shifts can be measured quite accurately, thereby determining the refractive index change. This "Fabry-Perot" interferometer had a slight tilt between the mirrors (a "wedge mode") producing almost straight fringes. The slight curve in the center of the fringes was due to distortions in sealing the flats. This cell was illuminated by a He-Ne laser beam of nearly monochromatic light made plane-parallel by a spatial filter and collimator and was made incident perpendicular to the first mirror by autocollimation. The spacing was adjusted by three nylon rods that could be pushed in to engage the differential screws and then pulled out, clear of the cell and shield so that no heat loss occurred down these rods.

Temperature Control

In these experiments, both cells and shields were temperature controlled. The controllers on the shields were DC bridges capable of controlling to ± 0.5 mK over twenty-four hours as tested in a well-stirred oil bath. The DC bridge is basically a Wheatstone bridge with the error signal being amplified by an op-amp and fed back by way of a power amplifier to the heater (see Figure 5). The

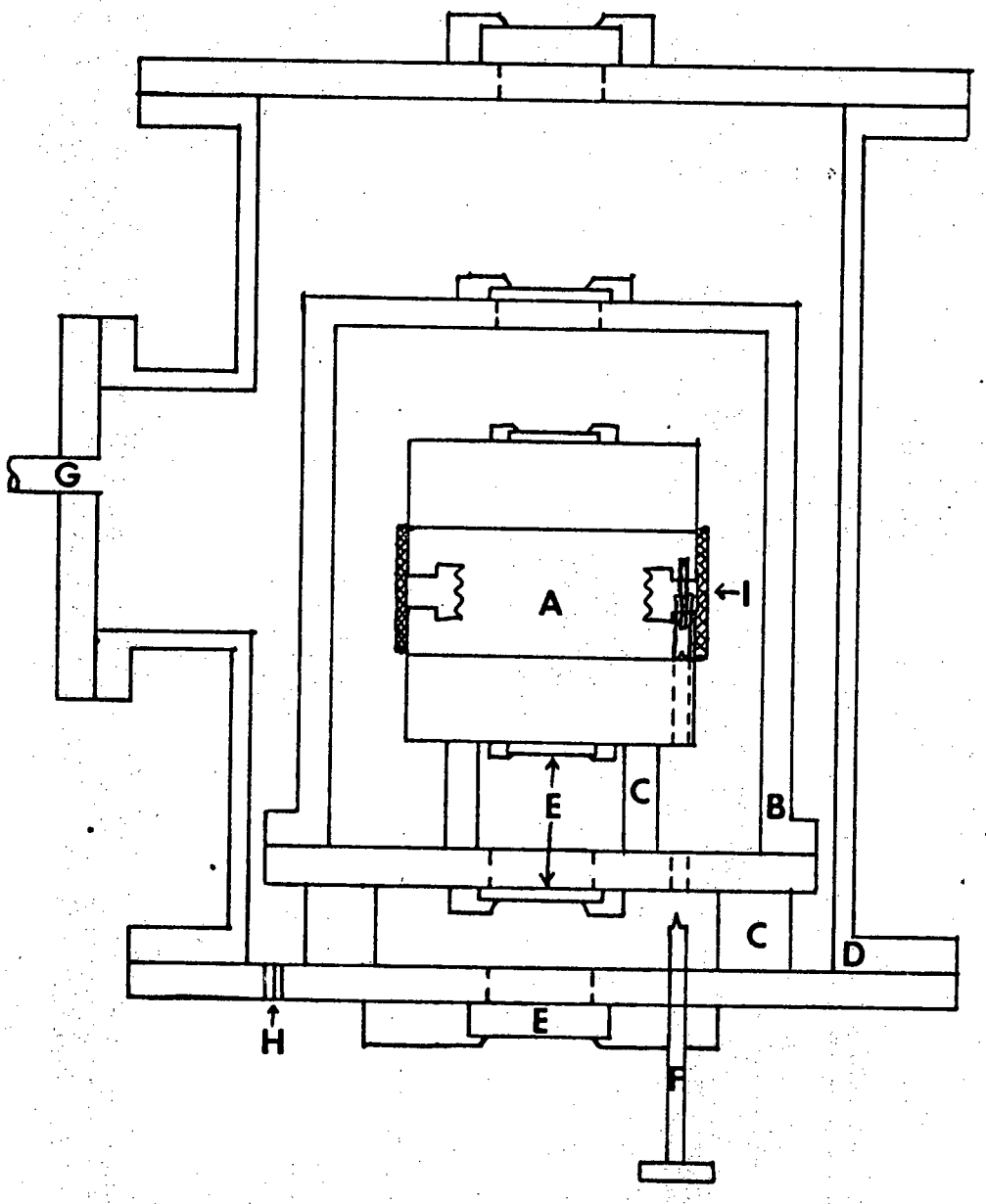

Figure 4: The variable spacing cell, A, is attached by nylon legs, C, to a surrounding aluminum heat shield, B. The heat shield is enclosed in vacuum jacket, D. Light passes through the windows, E. The spacing can be adjusted by the sliding nylon rods, F, engaging the differential screws. The vacuum pump is attached at the port, G. H is the electrical feedthroughs, and I is the braid used to provide a thermal path between the cell halves.

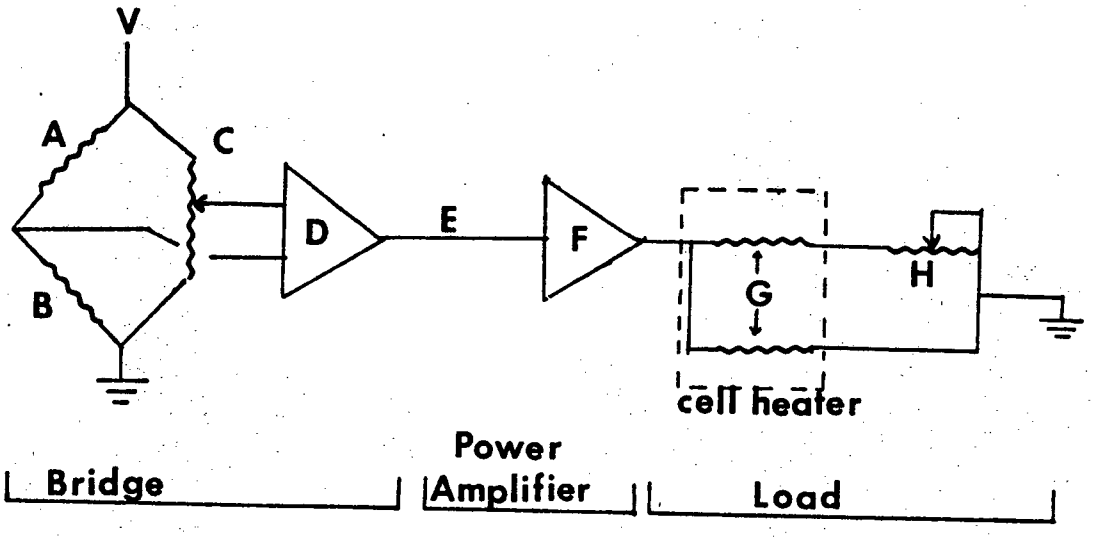

Figure 5: Schematic diagram of the temperature control system. The thermistor, A, and standard resistor, B, are basically in a Wheatstone Bridge which is balanced with the Kevin-Varley divider, C. The bridge unbalance is amplified at D with the error signal, E, being amplified by the power amplifier, F, which supplies power to the load. The load shown here is for the variable spacing cell where G are the heaters in the cell caps and H is the external trimpot used to eliminate temperature gradients.

thermistors (temperature sensitive resistors) used were "aged" (i.e., cycled several times from room temperature to operating temperature) Yellow Springs Instrument (No. 44004: 2250 ohm at 25°C) thermistors. (The stability and reliability of these thermistors is discussed in a later section.) The auxiliary thermistor used in the prism cell was calibrated after the experiment with respect to a standard platinum resistance element that had been calibrated by the National Bureau of Standards. The critical temperature found by this thermistor on the fluid sample in the prism cell was 45.474 ± 0.015 C, which differs from reported values of 45.14 ± 0.01 C by an amount consistent with the water impurity present in our fluids. Impurity effects will be discussed in a later section. This value of the critical temperature is consistent with the determination from the variable-spaced cell where absolute temperatures were known to only ± 0.2 K.

A separate DC bridge was used for temperature control of the prism cell allowing ± 2.5 mK control over twelve hours with the shield controlling to ± 10 mK over the same period of time. The variable spaced cell utilized a more sophisticated AC Kelvin bridge designed by Lyons (1973) that allowed a resolution of 20 μK and control of ± 50 μK per day. Since the room temperature was controlled to ± 0.2 K for this cell, the shield could control to ± 2 mK for periods of a week.

Experimental Precautions

In taking measurements of this kind there are several precautions that should be taken to insure that the interpretation of the data is correct. Since thermistors are used to monitor and control the temperature, they should be shown to be stable or at least to have only a small drift. Also, some assurance needs to be made on the resistance versus temperature curves supplied with the thermistor, not so much for absolute as for relative calibration. Some determinations as to the effects of gravity on the data and the size of their effects in binary fluids also should be made. Consideration of the predicted and observed effects of impurities should be made. Finally, a method to monitor and eliminate temperature gradients should be devised.

Thermistor Stability

Our thermistors were monitored while some preliminary data was being taken with the Fabry-Perot cell. There were four thermistors in the cell, one control and three auxiliary thermistors, and all were monitored. The three auxiliary thermistors were compared to each other after a long period of time (three months) to determine the long term drifts of the thermistors. A typical set of data (neither the best nor the worst) is shown in Figure 6. The drift with time was typically a millidegree per month. There was also a slight discrepancy in the relative temperature shifts given by the thermistors--an effect that was about 0.1% of the temperature change. Since all our temperatures were measured with respect to the critical temperature, this small error was not important unless

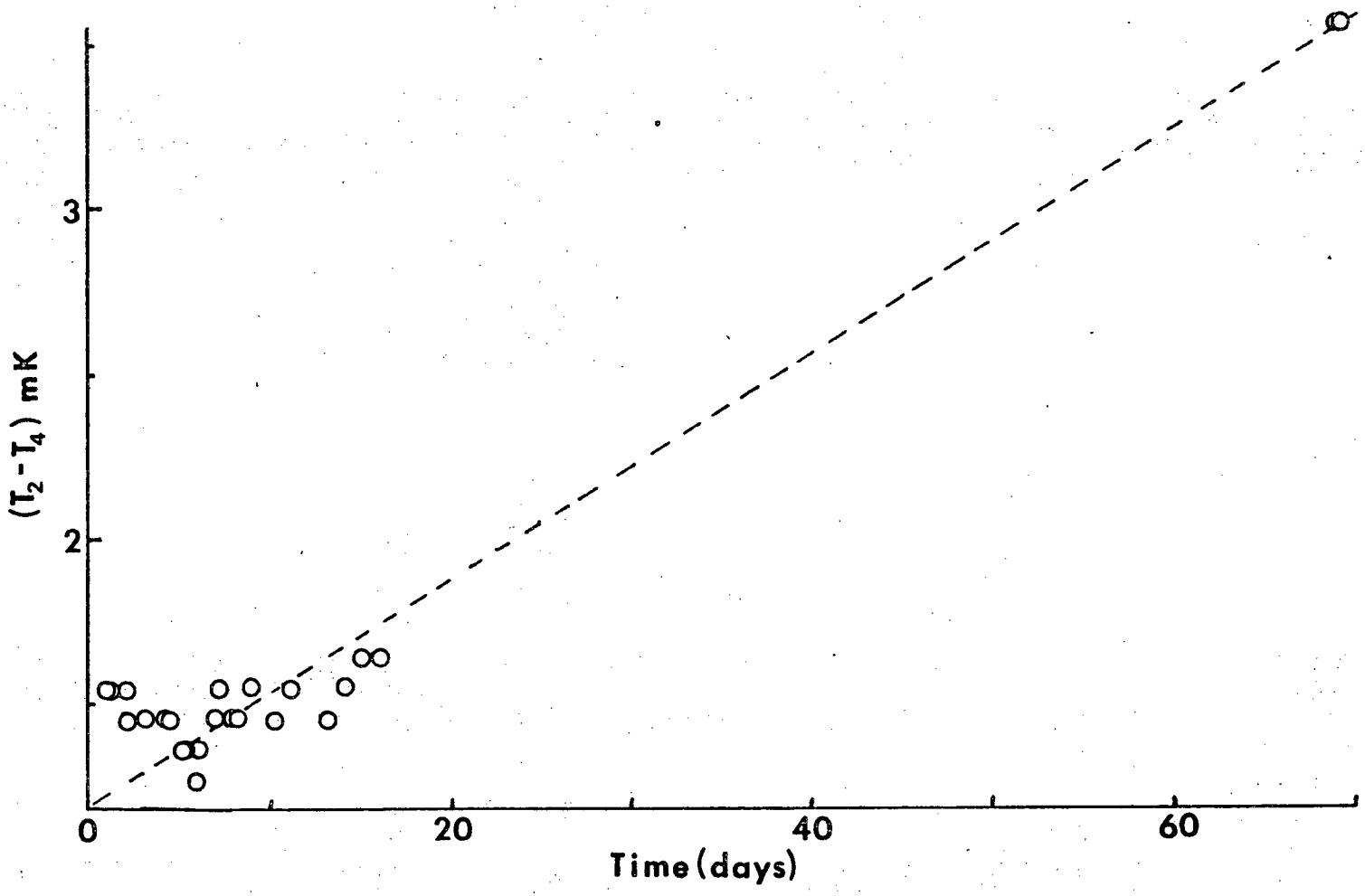

Figure 6: Thermistor drift with time at a constant temperature. $T_2 - T_4$ is the difference in the temperature readings of the second and forth thermistors.

far from the critical temperature (that is, more than 1°C). When compared with the critical temperature the thermistors were found to be consistent to within 1.5 mK over a period of about two months. The net effect was that the thermistor values could be trusted and that only over very extended regions in temperature was it necessary to worry about the temperature scale error. Thus, for the experiment in which the bulk coexistence curve over an 18°C range was measured, an auxiliary thermistor was calibrated at the completion of the experiment (the temperature intervals agreed to 0.03%). Because the slope of plots of the change in an effect versus the change in temperature usually gives the critical exponents, any error in the temperature scale is propagated directly to the critical exponents. One is fortunate to determine a critical exponent to 1% and so the small (0.1%) temperature scale error was not very significant.

In order to determine the temperature from the resistance of the thermistor, an equation must be fit. The equation that is generally recognized as providing the best fit with the fewest parameters is (Steinhart and Hart, 1968)

$$T^{-1} = A + B \log R + C [\log R]^3$$

where T is the absolute temperature and R is the corresponding resistance. This formula was used in the calibration procedure and in determining the temperatures of the other thermistors and is accurate to the extent described in the preceeding paragraph.

Gravity Effects

For a long time it was believed that the effects of gravity on a binary fluid mixture were negligible due to the very small compressibility of liquids. However, it is possible for the more dense component to slowly diffuse toward the bottom of the cell, and recent calculations (Fannin and Knobler, 1974) have shown that the effects can be as large as with pure fluids. Also, some recent experiments (Lorentzen and Hansen, 1966; Bagoi, et.al., 1970; Greer, et.al., 1975; Giglio and Vendramini, 1975) have observed a gravity effect in binary fluids. Fannin and Knobler (1974) have shown that gravity effects cause the data to curve up (to a smaller value of β) when close to the critical temperature as shown in Figure 7. How close the critical temperature can be approached before gravity effects become significant scales with the critical temperature, sample height and density difference of the two components (Fannin and Knobler, 1974). For example, they show that the effect is significant (0.2% of $(X - X_c)/X_c$; X = mole fraction) for the coexistence curve when $\epsilon = (T_c - T)/T_c \doteq 5 \times 10^{-4}$ for the mixture CH_4-CF_4 ($|\rho_1 - \rho_2|/\bar{\rho} = 1.38$) in a cell 2 cm high. For our fluids ($|\rho_1 - \rho_2|/\bar{\rho} = 0.016$) in a cell one cm high with a critical temperature one-third of theirs, the gravity effect would not become significant until the temperature was closer than 0.5 mK of the critical temperature. Thus, the critical temperature must be approached much closer than it was in these experiments to observe gravity effects for our fluids, methanol-cyclohexane.

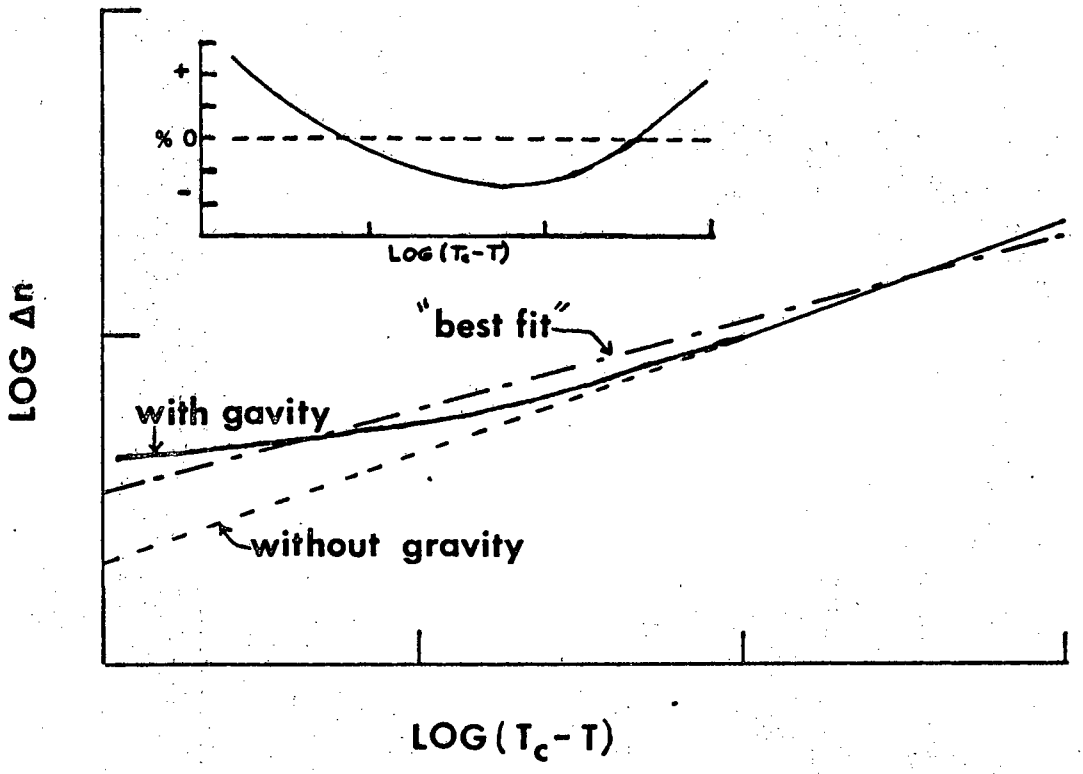

Figure 7: Gravity effects on the coexistence curve. The dashed line represents a system without gravity effects. Gravity causes the data to deviate as shown in the solid line so that a best fit to the data (dot-dashed line) has a different slope than with the gravity effects taken into account (dashed line). The inset shows how the residuals (the deviation of the best fit from the data) reflect the poor fit and indicate a correction is necessary to properly fit the data.

Impurity Effects

Early research on this binary fluid mixture was done to determine the effect of various impurities on the critical temperature and coexistence curve. Jones and Amstell (1930) introduced water as an impurity to provide a guide in preparing pure methanol, which is very hygroscopic. Later, Eckfeldt and Lucasse (1943) used inorganic salts as an impurity and showed, in agreement with Jones' work, that the binary mixture methanol-cyclohexane is much more sensitive to a water impurity. (A 0.003% water impurity is quoted as causing an increase in the critical temperature of 0.05 K.) Eckfeldt and Lucasse (1943) also state that the effect of water on the critical temperature is more than ten times that for organic impurities. Unfortunately, systematic measurements to determine the impurity effect of water on our system (giving both the critical temperature and exponent dependence) have yet to be done. However, experiments on this mixture (Warren and Webb, 1969) and other mixtures (Bak and Goldburg, 1969; Bak, Goldburg and Pusey, 1970; Goldburg and Pusey, 1972) indicate that although the critical temperature may shift due to a small impurity, the critical exponents, measured relative to the shifted critical temperature, do not seem to change significantly.

In the experiments described here, the various sample cells were prepared with fluids from the same bottles. The fluids used were Fisher "Spectranalyzed" methanol (99.95% pure) and cyclohexane (99.98% pure) with the major impurity in each being water. This resulted in a 0.3% by weight water impurity in our sample cells. Rather than undertake the questionable task of further purifying

the fluids, emphasis was placed on preventing introduction of additional impurities when filling the cell. The cells were thoroughly cleaned and then placed in an oven to remove any residual moisture. The hot cell was then placed in a dry nitrogen atmosphere until filling. Loading the cell with the fluids occurred in the same dry box using phosphorous pentoxide as a dessicant and under a constant stream of dry nitrogen. Massing of the cell took place outside this box with the cell sealed after the filling of each component. The concentration of fluids was thus known and kept close to the quoted critical value, which was checked in the coexistence curve experiment. Samples prepared in this manner gave consistent values for the critical temperature and suggested that further impurities were not introduced on filling.

Since it has been experimentally observed and theoretically predicted (Kouvel and Fisher, 1964) that the critical exponents do not significantly (< 2%) change their values for small amounts of impurities, then the only concern rests on the impurity effects of the critical temperature dependence on film thickness. Although a critical exponent should describe this behavior (Fisher, 1971), further assurance should be provided. Since this is the first experiment done on such a dependence, no experimental data are available on impurity effects. However, Ising model calculations have been done, assuming random lattice impurities, by Miyazima (1973) in which the critical temperature dependence on film thickness was found not to alter for small impurity concentrations.

We use this theoretical prediction to justify our tolerance of the small (0.03% by weight) water impurity used in this work.

Temperature Gradients

For the variable-spaced cell (see Figures 3 and 4), the temperature gradient across the cell could be adjusted by means of an external trimpot connected in series with the heater coil remote from the nylon supports. Such an adjustment was needed since the nylon support legs, which were on one side of the cell, conduct some heat. This heat loss can be compensated by externally dissipating an equivalent amount of the energy that would power the other side of the cell. The two heater coils were matched in resistance to 0.1 Ω and connected in parallel to the power amplifier (see Figure 5).

The size of the gradient (if one exists) depended, in this case, on the temperature difference between the cell and shield. To determine if such a gradient was present, a thermistor on each cell half (not necessarily calibrated with respect to each other) was monitored while the temperature difference between the cell and shield was varied (see Figure 8). A gradient was present if the temperature difference between the two cell halves changed as the temperature between the cell and shield changed. The value at which the external trimpot should be set to eliminate a gradient was determined from two values of the temperature difference between the cell and shield as the trimpot setting was varied. These data form two straight lines when plotted with the temperature difference across the cell versus the fraction of power

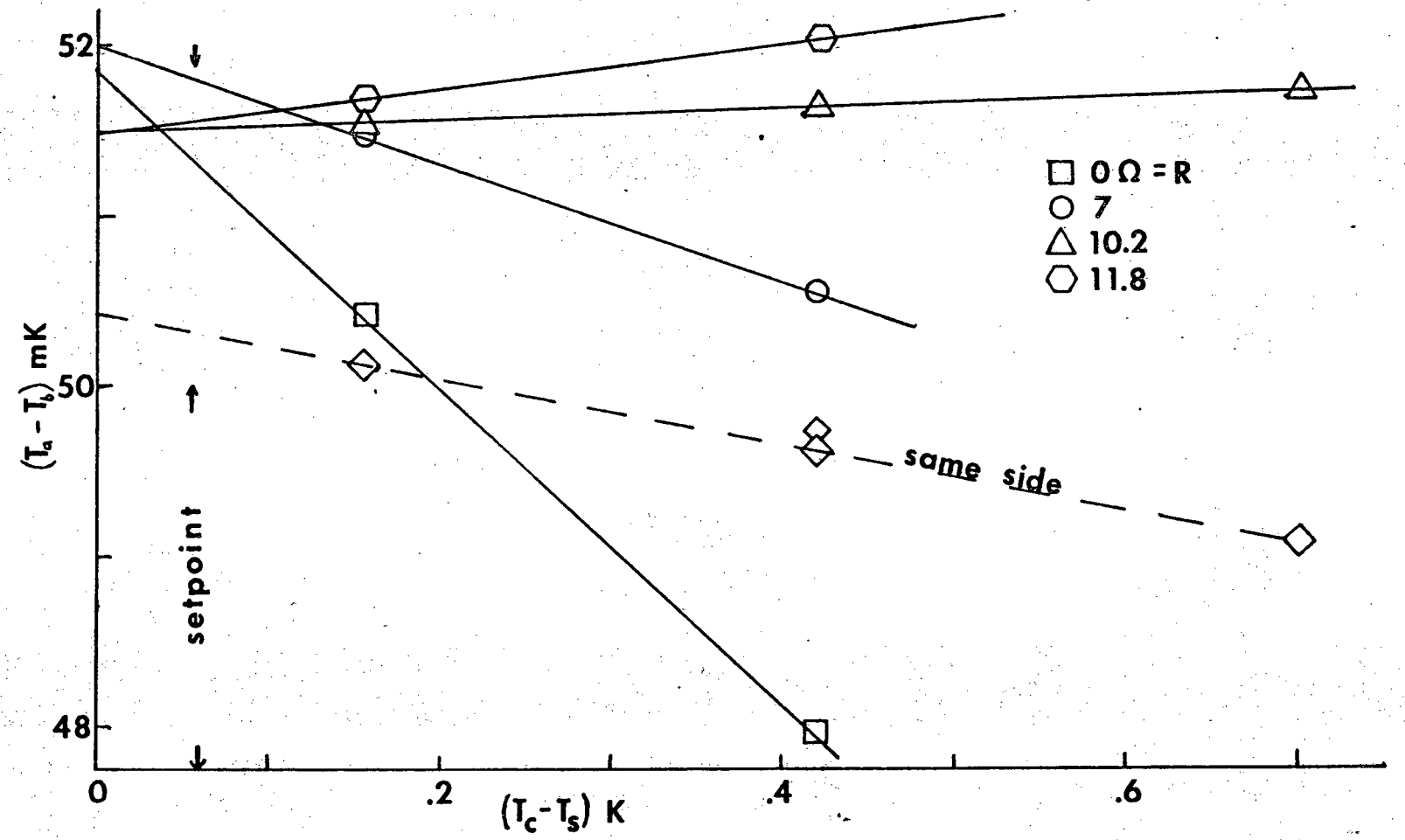

Figure 8: Temperature Gradients. The temperature difference across the cell, $T_5 - T_6$, was monitored while the temperature difference between the cell and shield, $T_c - T_s$, was varied at a fixed trimpot resistance, R (solid lines). The dashed line was $T_2 - T_6$, the temperature difference between two thermistors on the same cell half, as a function of $T_c - T_s$.

dissipated in the trimpot; the intersection gives the value of the trimpot needed to offset the heat conduction through the nylon supports (see Figure 9). This value allowed the two cell halves to be the same temperature independent of the cell and shield temperatures and without having previously calibrated the two thermistors.

Two additional points should be made concerning this adjustment. First, an additional thermistor mounted on the same side as the nylon posts indicated a slight gradient around the cell half (the two thermistors were at the perimeter and about 90° apart) as seen in the dashed line in Figure 8. This gradient was presumably caused by the screws on the clamps holding the braid in place radiating slightly more than the uniform body and was kept to $\sim$ 0.1 mK by keeping the shield temperature close to the cell temperature ($T_c - T_s \simeq 0.06°C$). Secondly, the gradients measured were quite small and could be buried in the uncertainty of measurement if one tried to, for instance, calibrate two thermistors and then separate them. The method described here is certainly the easiest and appears to give very satisfactory results.

With the prism cell, no adjustments were possible but a measurement indicated that the temperature gradient was less than 2.5 mK (the measurement accuracy) across the cell. Temperature gradients could be visually observed as convection currents in the cell. This was not observed in this bulk coexistence curve experiment.

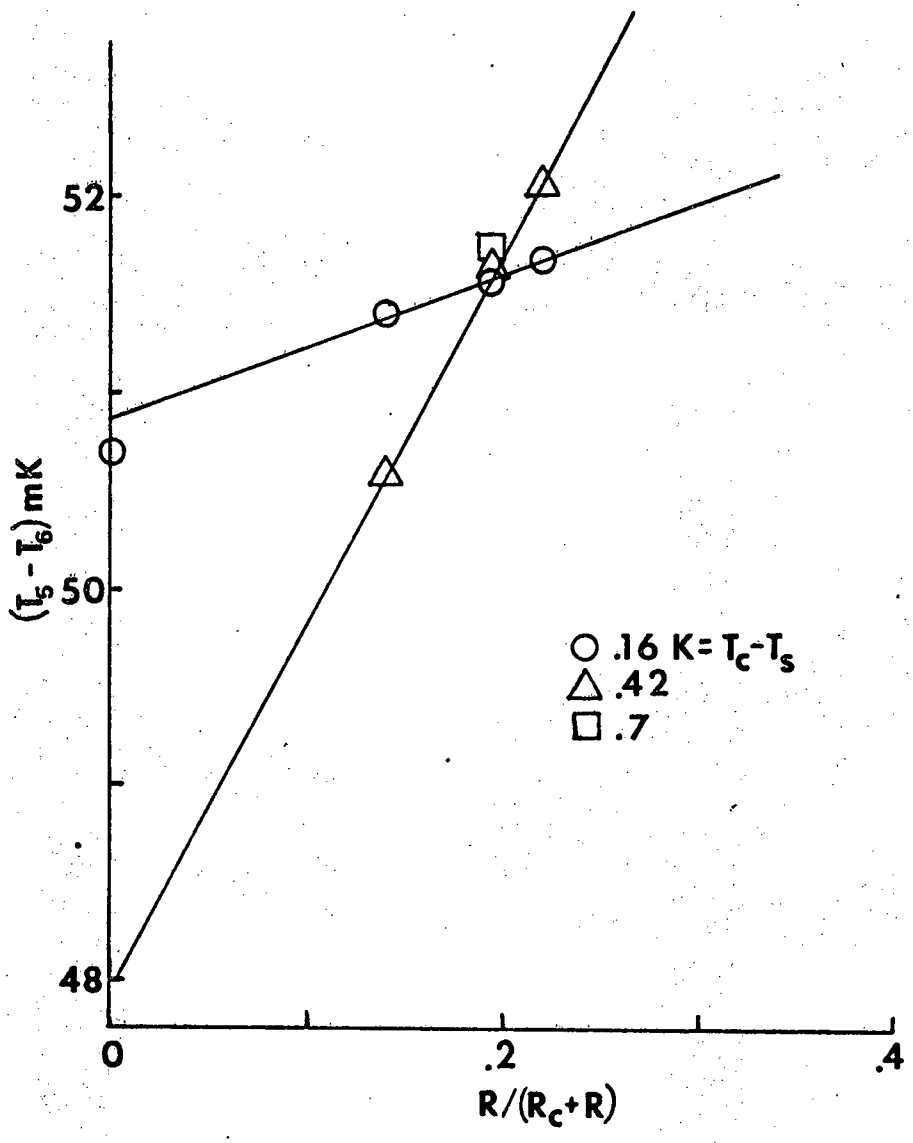

Figure 9: The temperature difference across the cell, $T_5 - T_6$, as a function of the fraction of power dissipated in the trimpot at fixed values of $T_c - T_s$. R is the resistance of the trimpot and $R_c = 40\ \Omega$ is the resistance of a heater coil. The lines intersect at the optimum setting of R ($\simeq 10.2\ \Omega$).

CHAPTER III

EXPERIMENTAL PROCEDURE AND RESULTS

Introduction and Lorentz-Lorenz Relation

In doing refractive index measurements to probe critical phenomena, it is often necessary to relate the refractive index to density or volume fraction. Hartley (1974) has shown that the standard and well-accepted Lorentz-Lorenz formula $(n^2 - 1)/(n^2 + 2) = 4\pi\alpha\rho/3$, where α is the polarizability and ρ is the mass density, approximately holds for the background (non-fluctuating) refractive index of a binary fluid mixture. However, in applying this to critical phenomena, some care must be taken that the anomaly in the refractive index and in the density (or volume) near the critical point does not invalidate the relation. Although the refractive index anomaly has already been measured for this system by Hartley (1974), he did not use the critical concentration and may have underestimated the size of the anomaly. For this reason and to try to obtain more precise data, the refractive index anomaly measurements on this system were repeated. The density anomaly is predicted to be very small (Fannin and Knobler, 1974) and is difficult to measure. We looked for such an effect when the coexistence curve was measured even though preliminary results by Scheibner (1976) showed the effect to be too small to be seen, even with the differential

refractometer. The anomalous refractive index measurements are discussed by Hartley and shown to be less than 10^{-4}. This is less than the error of measurement in the other experiments so that the Lorentz-Lorenz relation can be applied to these (coexistence curve) measurements. The Lorentz-Lorenz relation will now be applied to the bulk coexistence curve data.

Bulk Coexistence Curve

It was shown by Hartley(1974) that the refractive index anomaly is less than 1×10^{-4} when $T - T_c > 1$ mK so that the measurements of the bulk refractive index can be used to probe the critical fluid's behavior. By using refractive index techniques to measure the coexistence curve, in the manner described below, both the shape of the "rectilinear" diameter (mean density) and the coexistence curve (giving the critical exponent, β) can be determined. These data will be compared with other measurements determining β in pure fluids and binary mixtures to see if these systems have the predicted value of β given by the three-dimensional Ising model.

As was alluded to in Appendix A, the nonlinear operators in Renormalization Group Theory will cause corrections to simple scaling (Wegner, 1972). In particular, this corrections-to-scaling approach has recently been found to be important for coexistence curves, particularly in pure fluids (Hocken and Moldover, 1976; Greer, 1976). The correction would be expected to be more easily seen for the coexistence curve since data can be

taken for very large values of $|T - T_c|$. The coexistence curve data presented below will be analyzed with such corrections in mind.

The coexistence curve of methanol-cyclohexane was first studied by Lecat (1909) and then by Jones and Amstell (1930) and Eckfeldt and Lucasse (1943), where the effect of impurities was considered. The only recent studies have been done by Gilmer, et.al., (1965) and Campbell and Kartzmark (1967), both of whom also used a refractive index technique. However, these works were not extensive enough to even determine the critical exponent, β, much less answer the questions posed above and so this first experiment was undertaken.

For some time a disparity has existed between the critical exponent describing the coexistence curve of pure fluids (Sengers, 1975; Sengers, Greer and Sengers, 1976) ($\beta = 0.355 \pm 0.007$) and that for binary mixtures (Stein and Allen, 1974) ($\beta = 0.34 \pm 0.01$) with the series expansion result for the Ising (lattice-gas) model (Domb, 1974) ($\beta = 0.313$). However, recent measurements on pure fluids (Estler, Hocken, Charlton and Wilcox, 1975; Hocken and Moldover, 1976) and binary mixtures (Balzarini, 1974; Greer, 1976) show that by taking gravity effects (Fannin and Knobler, 1974) and a correct form for extended scaling (Greer, 1976) into account, these values of β for pure fluids ($\beta = 0.320 \rightarrow 0.329$) and binary mixtures ($\beta = 0.322 \rightarrow 0.328$) agree with recent Renormalization Group calculations (Kadanoff, et.al., 1976; Baker, et.al., 1976) for the Ising model ($\beta = 0.322 \pm 0.002$) and are much closer to the old series expansion value. We point out that for our system,

which has been shown to be virtually free of gravity effects, a value of $\beta = 0.326 \pm 0.003$ is determined with only simple scaling needed to fit the data ($\varepsilon < 0.06$).

To take the data on the coexistence we measured the refractive index of the fluids by capturing them in a fluid prism as described earlier. The relation between the refractive index, n, and the measured angles is the elementary one for a simple prism: $n = \sin [(\psi - \psi_0 + \theta)/2] / \sin (\theta/2)$ where θ is the prism angle, ψ_0 is the undeviated angle and ψ is the minimum deviated angle (see Figure 2). Because of the large windows on the cell, the usual methods of determining the prism angle were not possible. However, by placing the cell on the stage and fixing the telescope while allowing the table to rotate, the prism angle could be determined by autocollimation. A He-Ne laser beam struck the prism perpendicularly at the axis and with a separation of about eighteen feet between them. The beam could be reflected from the first (which overlapped with the second) surface back into the laser aperture with an error of $\pm$ 3 mm (which corresponds to an error of 10 sec of arc). By repeating these measurements for each window, the prism angle was determined to be $60.156° \pm 0.005$. The remaining measurements were taken with the table fixed and the telescope free to rotate. With the prism cell removed, the undeviated angle was measured and checked occasionally. (Although this quantity should remain constant, there was sufficient play in the telescope assembly to rotate the telescope if the eyepiece was handled when moved to the next position.) A vintage J. W. Queen & Co. spectrometer with an eleven and a half inch base was used, allowing a

resolution of 10 secs of arc. The cell was placed on the table at a position which compensated for the shift of the light due to the half-inch thick window. (A shift does not alter the measured deviated angle since the glass surfaces are flat and parallel.) We measured the minimum deviation angle, ψ, for each line several times with a precision of less than 10 secs of arc. We estimate the error in refractive index due to the uncertainties in measurement (errors in prism, undeviated and deviated angles as well as non-parallel window surfaces) to be $\pm$ 0.00015.

Because of the recent observations (Lorentzen and Hansen, 1966; Bagoi, et.al., 1970; Greer, et.al., 1975; Giglio and Vendramini, 1975) of density gradients due to gravity in binary fluids, we started our experiment by looking for such gravity effects, although they are predicted to be very small for our system due to the closely matched densities (see previous comments in Experimental Precautions). After our system had been at room temperature for some time with the slit source images (which I call "lines") straight, we raised the temperature a few degrees and noticed some curving of the lines near the meniscus for many hours after the new temperature had been reached. We discovered that this was due to concentration gradients in the cell caused by the slow diffusion across the meniscus and not a density gradient others (Lorentzen and Hansen, 1966) have reported using a similar technique. The meniscus was also observed to persist well above the critical temperature. We found no curving of the lines even very close to the critical temperature ($T - T_c < 5$ mK) if the cell was shaken after temperature equilibrium had been reached.

Shaking the cell did not affect the deviated angle of the line within our precision of measurement. We have also looked for the characteristic sigmoid shape of the gravity effects using a "Fabry-Perot" interferometer in the wedge mode, but have been unable to detect any above or below the critical point even after waiting several days. However, small temperature gradients may have inhibited the formation of this effect.

Data Collection

The minimum deviated angle was measured several times, after which the temperature was changed and allowed to come to equilibrium before shaking the cell. The time span between shaking and taking the next set of measurements depended on how far from the critical temperature the cell was, but typically the wait was from four to twelve hours. The critical point was defined as the temperature at which the meniscus would just appear or disappear after shaking the cell and allowing it to stand for several hours. Although strong opalescence was encountered near the critical point, we were still able to take reproducible measurements within 5 mK of the critical temperature, which was determined to ± 2.5 mK. After about twenty-five points were taken, some pump oil condensed on the cell and shield. To remove this contaminant, the sealed cell was placed in a vapor degreaser for a few seconds; however, this resulted in a shift of 110 mK in the readings of the controlling thermistor relative to the critical point. An auxiliary thermistor imbedded deep in the cell body showed no change in the critical temperature, so the fluids were not contaminated. Since

all of the data agree whether taken before or after this occurrence or while raising or lowering the temperature, we make no distinction in presenting it in Table II in order of increasing $T_c - T$.

Although visual observation could determine the critical temperature to ± 2.5 mK, a more precise value could be determined by using the method of Kouvel and Fisher (1964). By assuming scaling and constructing the numerical derivative from the data taken below T_c, the quantity $T^* = [(d(\Delta n)/dT)/\Delta n]^{-1} = (T_c - T)/\beta$ can be constructed allowing a determination of T_c (independent of β) to ± 0.5 mK and to a value consistent with that observed visually (see Figure 10). We will show in the next section that the scaling assumption used above is not violated over the temperature range measured with this mixture.

Data Analysis

From the refractive index data taken above and below T_c, we can determine the shape of the coexistence curve, the critical concentration and the rectilinear diameter. The average of the refractive indices above and below the meniscus is a measure of the mean density of the fluid and is called the "rectilinear" diameter of the coexistence curve (see Figure 11). A straight line drawn through the data points above T_c intersects the "rectilinear" diameter at a point on the coexistence curve indicating that we are very close to the critical concentration. (The diameter of the coexistence curve fit very well to a straight line of the form $(n_U + n_L)/2 = A + B'(T_c - T)$ with $A = 1.37956$ and $B' = 2.96 \times 10^{-4}/K$. See Figures 11 and 12a.) The rectilinear

TABLE II

BULK COEXISTENCE CURVE DATA

$(T_c - T)K$	n_U	n_L	$n_U - n_L$	$(n_U + n_L)/2$
- 3.436	1.37765			
- 2.403	1.37825			
- 1.363	1.37888			
- 0.661	1.37926			
- 0.241	1.37951			
0.0026	1.38155	1.3785	0.00305	1.38002
0.0074	1.38222	1.3774	0.00482	1.37981
0.0094	1.38218	1.37743	0.00475	1.3798
0.012	1.38233	1.37692	0.00541	1.37962
0.0124	1.38239	1.37677	0.00562	1.37958
0.0294	1.38292	1.3765	0.00642	1.37971
0.036	1.38307	1.37562	0.00745	1.37934
0.0484	1.38354	1.37575	0.00779	1.37964
0.0654	1.38406	1.37536	0.0087	1.37971
0.084	1.38429	1.3744	0.00989	1.37934
0.0864	1.38473	1.37484	0.00989	1.37978
0.094	1.38442	1.37411	0.01031	1.37926
0.1104	1.38494	1.37431	0.01063	1.37962
0.171	1.38557	1.37327	0.0123	1.37942
0.182	1.38612	1.37316	0.01296	1.37964
0.209	1.38644	1.37317	0.01327	1.3798
0.305	1.38676	1.37194	0.01482	1.37935
0.406	1.38745	1.37124	0.01621	1.37934
0.502	1.38804	1.37067	0.01737	1.37935
0.579	1.38849	1.37022	0.01827	1.37935
0.67	1.38912	1.37001	0.01911	1.37956
0.694	1.3891	1.36962	0.01948	1.37936
0.797	1.3895	1.36923	0.02027	1.37936
0.916	1.39025	1.36887	0.02138	1.37956
0.923	1.39013	1.36877	0.02136	1.37945
1.167	1.39106	1.36802	0.02304	1.37954
1.799	1.39348	1.36693	0.02655	1.3802
2.749	1.3959	1.36506	0.03084	1.38048
3.792	1.39762	1.36369	0.03393	1.38065
4.686	1.39849	1.36263	0.03586	1.38056
5.59	1.40014	1.36171	0.03843	1.38092
6.573	1.40169	1.36086	0.04083	1.38127

TABLE II (continued)

BULK COEXISTENCE CURVE DATA

$(T_c - T)K$	n_U	n_L	$n_U - n_L$	$(n_U + n_L)/2$
7.645	1.40297	1.36029	0.04268	1.38163
8.656	1.40434	1.35987	0.04447	1.3821
9.451	1.40534	1.35959	0.04575	1.38246
10.329	1.40606	1.35909	0.04697	1.38257
11.312	1.40729	1.35891	0.04838	1.3831
12.423	1.40818	1.35835	0.04983	1.38326
13.265	1.40904	1.35806	0.05098	1.38355
14.126	1.40955	1.35771	0.05184	1.38363
15.183	1.4107	1.35752	0.05318	1.38411
16.212	1.41167	1.35721	0.05446	1.38444
17.207	1.41249	1.35704	0.05545	1.38476
18.205	1.4132	1.35675	0.05645	1.38497

Figure 10: T^* versus $\overline{T}$ for one set of bulk coexistence curve data. The scatter in the data results from taking the numerical derivative of the Δn versus T data.

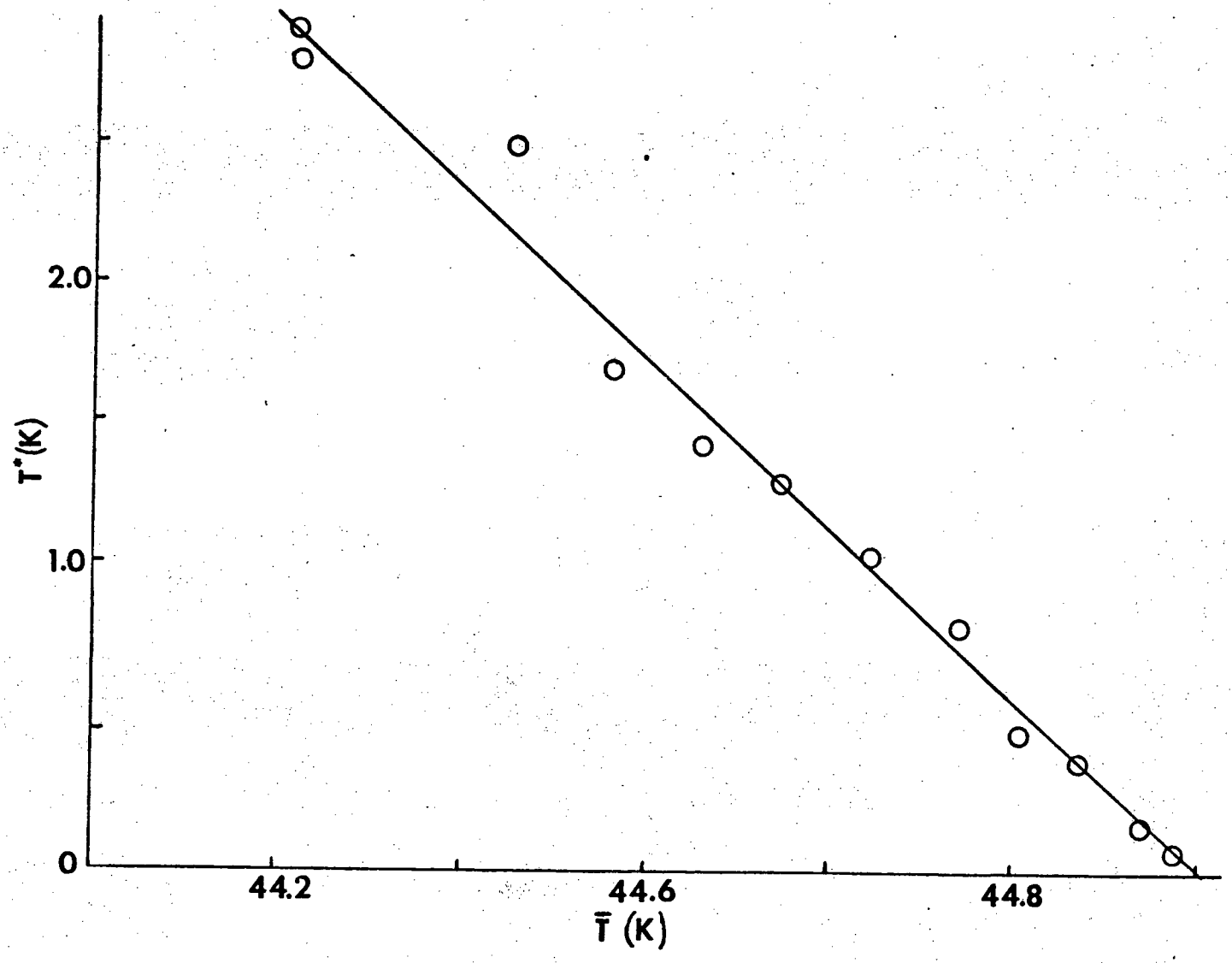
2.0
1.0
0
T*(K)
44.2
44.6
44.8
T̄ (K)

Figure 11: The coexistence curve of methanol-cyclohexane as given in Table II. The data above the critical temperature (T_c = 45.474°C) has a slope of 5.82×10^{-4}/°C and an intercept with the coexistence curve of 1.37966. The rectilinear diameter (average of the refractive index above and below the meniscus) is the solid squares and line bisecting the coexistence curve. The line is a least squares fit to $(n_1 + n_2)/2 = A + B'(T_c - T)$ with $A = 1.37956$ and $B' = 2.96 \times 10^{-4}$/°C and where n_1 and n_2 are the refractive indices above and below the meniscus respectively.

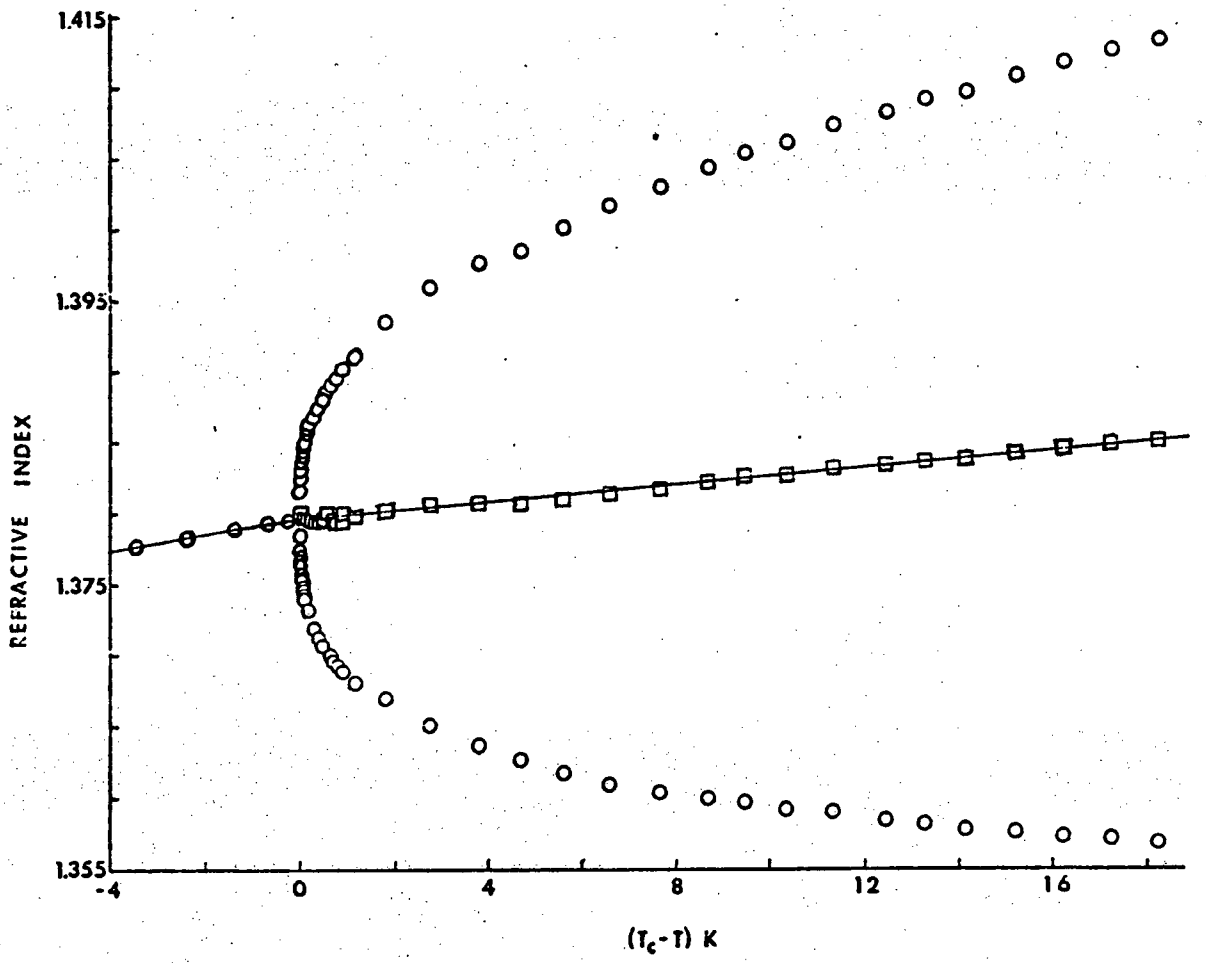
1.415
1.395
1.375
1.355
REFRACTIVE INDEX
-4
0
4
8
12
16
(T_c - T) K

Figure 12: The residuals from the fit to (a) the rectilinear diameter in Figure 11 and (b) our data in Figure 13. The residual is the amount the fitted line differs from the data point divided by the data point's error.

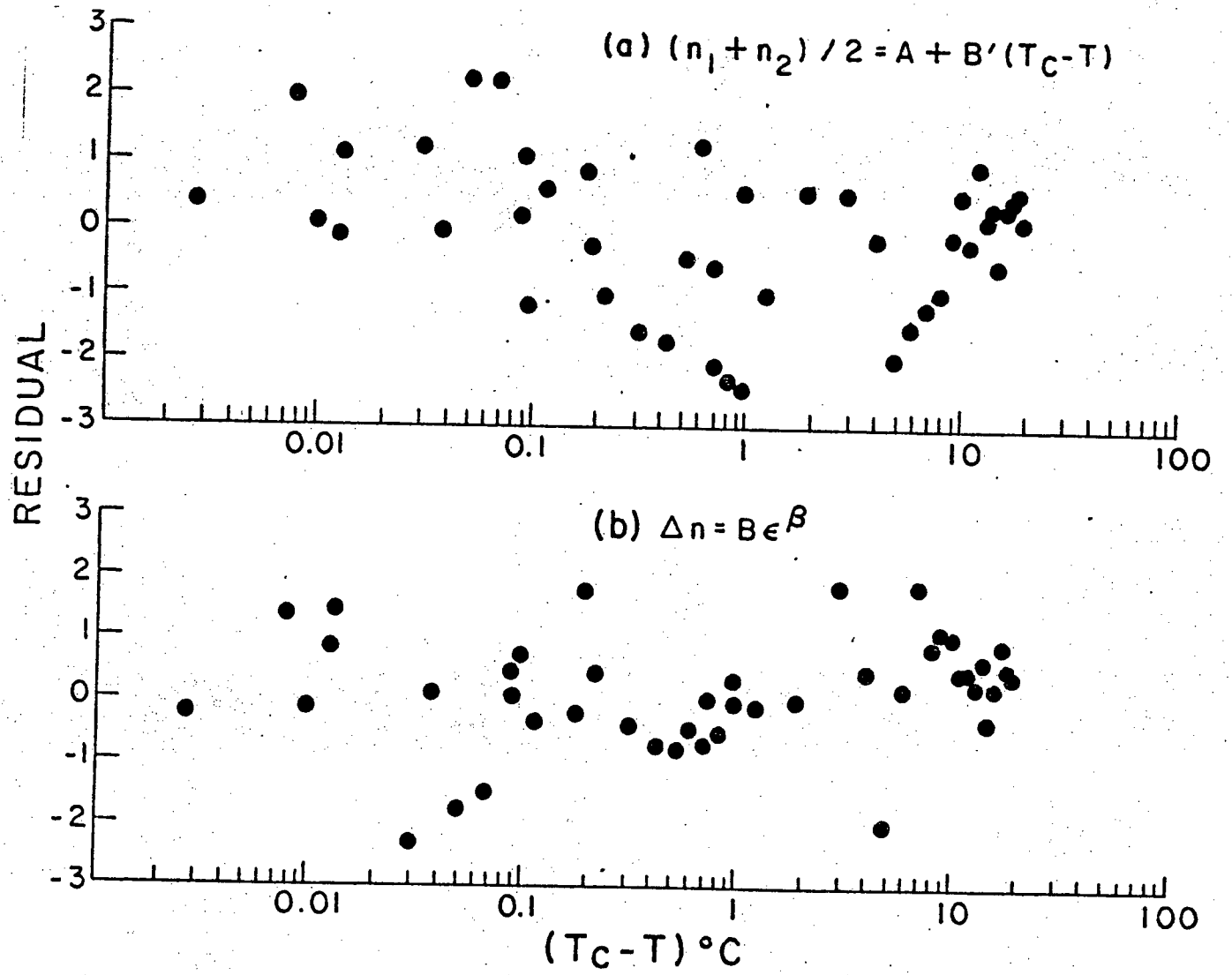
(a) $(n_1+n_2)/2 = A + B'(T_C-T)$
(b) $\Delta n = B\epsilon^{\beta}$
RESIDUAL
3
2
1
0
-1
-2
-3
0.01
0.1
1
10
100
(T_C-T) °C

diameter extrapolated to the critical temperature gives the critical refractive index to be 1.37956 ± 0.00005. From the data above the critical point the refractive index at the critical point is extrapolated to be 1.37966. So, by using the Lorentz-Lorenz relation, the critical concentration was determined from these two values of n at T_c to be 29.04 ± 0.1% by weight methanol.

It has been predicted (Hemmer and Stell, 1970 and 1972; Widom and Rowlinson, 1970; M.S. Green, et.al., 1971; Mermin and Rehr, 1971; Mermin, 1971a and 1971b) and observed (Weiner, et.al., 1974; Gopal, et.al., 1974) that the "rectilinear" diameter (mean density) has some sort of an anomaly near the critical point. However, this was not seen in this experiment (see Figures 11 and 12a).

The index of refraction of a mixture of liquids can be related to the volume fraction by the Lorentz-Lorenz relation

$$V(n^2 - 1)/(n^2 + 2) = 4/3\pi\sum_i \alpha_i M_i$$

where n is the index of refraction of the mixture, V is the total volume, α_i is the polarizability per unit mass of the i^{th} component and M_i is its mass. If we consider two components, then we have $(T > T_c)$

$$(n^2 - 1)/(n^2 + 2) = (n_1^2 - 1)/(n_1^2 + 2)\phi_1 + (n_2^2 - 1)/(n_2^2 + 2)(1 - \phi_1)$$

where n_1 (n_2) are the refractive index component 1 (2) and ϕ_1 (ϕ_2) is its volume fraction V_1/V (V_2/V). If one is below T_c then there is a volume fraction of component 1 in the upper (ϕ_1^U) and lower (ϕ_1^L) phases giving refractive indices n_U, n_L. If we define $A_i = (n_i^2 - 1)/(n_i^2 + 2)$, $i = 1, 2$, and solve the previous equation

for $\Delta\phi_1 = \phi_1^U - \phi_1^L$, we obtain

$$\Delta\phi_1 = K'(n_U - n_L) = K'\Delta n, \text{ where}$$

$$K' \equiv 3(n_U + n_L)/[(A_1 - A_2)(n_U^2 + 2)(n_L^2 + 2)].$$

The constant K' is only slightly temperature dependent. For our fluids a value $T_c - T = 18.205$ K gives $K' = 10.59$ where $T_c - T = 0$ gives $K' = 10.48$ (an error in K' of 1% over 18 K). The error in Δn ranges from 0.4% to 10% over the same 18 K temperature range. The small systematic error in assuming K' to be a constant is thus small compared to our experimental uncertainty, and Δn is proportional to $\Delta\phi_1$. (The 1% error in assuming K' a constant would increase the value of β by 1% if the data were plotted using $\Delta\phi_1$. I choose to present the Δn data keeping in mind this error.)

To analyze the coexistence curve and determine what the critical exponent β should be, a "properly" weighted least squares fit to our data, shown in Figure 13, is required. By "properly" weighted we mean that one needs (Sengers, 1975) to propagate the temperature error into the refractive index error bars and take into account that one is fitting a log-log scale and weight the points in the fit accordingly. We used the method described by Bevington (1969) to obtain the fit (shown in Figure 13) to the function $\Delta n = B\varepsilon^\beta$ with $\beta = 0.326 \pm 0.003$ and $B = 0.143 \pm 0.008$ (the errors are three standard deviations). It is important to use a properly weighted fit to the data and also to have a sufficient number of data points over the temperature region studied so one can say with reasonable accuracy what is the best

Figure 13: The difference in refractive index (proportional to the volume fraction) above and below the meniscus as a function of $T_c - T$. The open circles are the data taken in this experiment, the triangles (Δ) are from Hartley (1974) and the inverted triangles (∇) are from Gilmer, et.al., (1965). The line is a fit to our data using simple scaling, $\Delta n = B\epsilon^{\beta}$, with $\beta = 0.326 \pm 0.003$ and $B = 0.143 \pm 0.008$ (uncertainties are three standard deviations).

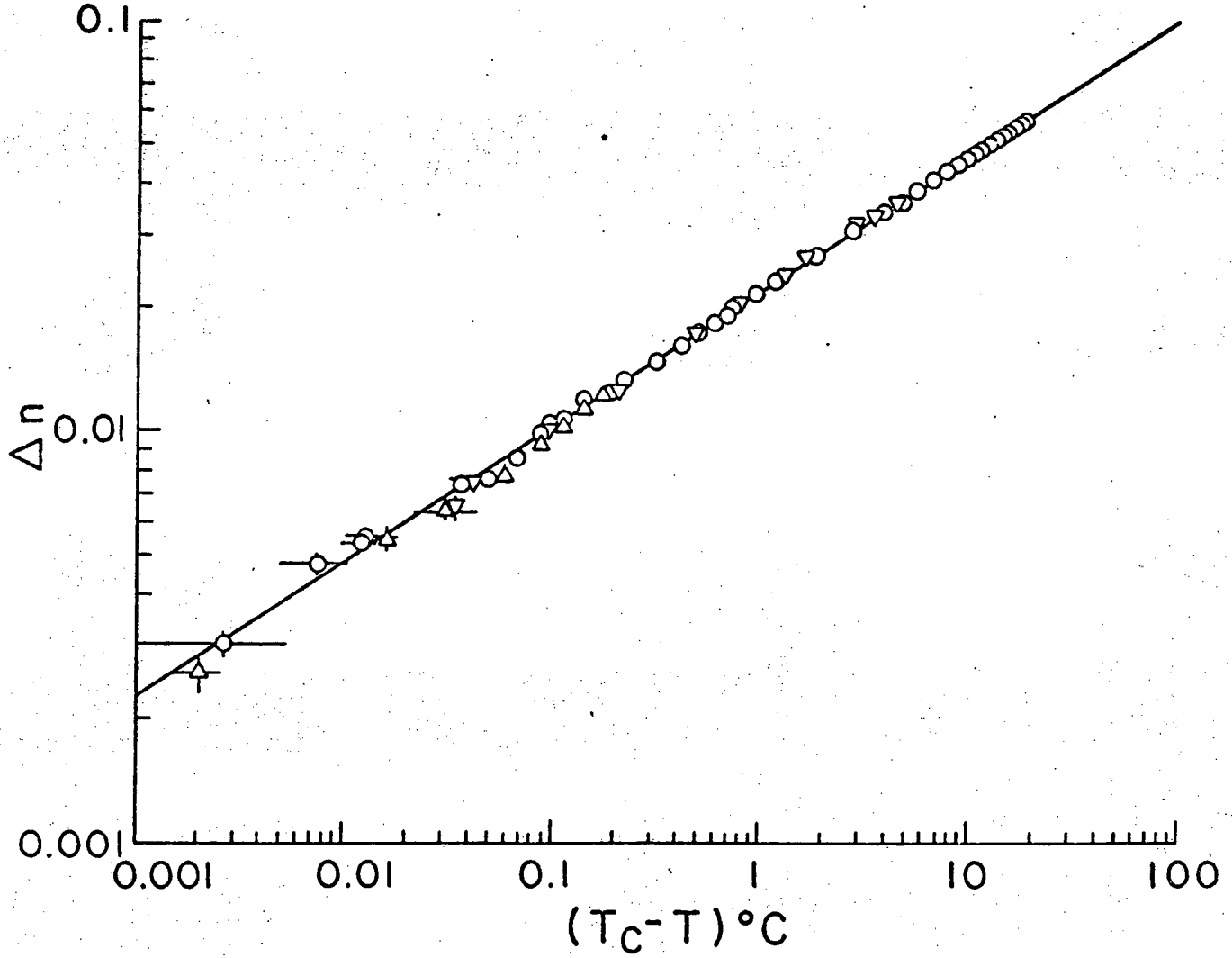
0.1
0.01
0.001
Δn
0.001
0.01
0.1
1
10
100
(T_C - T) °C

fit. Others (Gilmer, et.al., 1965; Hartley, 1974) who have measured the coexistence curve for methanol-cyclohexane using refractive index techniques have taken less data over a smaller temperature region and have found higher values for the critical exponent β (0.347 ± 0.008 and 0.35 ± 0.02). Their data are consistent with ours as shown in Figure 13.

Comments and Conclusions

It has been shown that refractive index techniques are a valuable probe into critical behavior and that the difference in refractive index between two phases is effectively the same as the difference in volume fraction--the preferred order parameter in coexistence curve measurements in binary liquid mixtures.

There has been recent evidence that corrections to scaling as predicted by Wegner (1972) are necessary for pure fluids and binary mixtures to explain the coexistence curve data. As seen in Figure 12b, a simple scaling relation works well for this data with correction terms not significantly improving the fit. (Greer (1976) states that the first correction term gives $\Delta n \doteq B\varepsilon^{\beta} + B_1\varepsilon^{\beta} + 0.5$.) With this correction term the weighted non-linear fit gives $B_1 \approx 2.5 \times 10^{-3}$ and a reduced chi squared of 0.76 versus 0.79 without a correction term ($B_1 = 0$). (The values of B and β are effectively the same whether $B_1 = 0$ or 2.5×10^{-3}.)) It has been suggested (Greer, 1976) that extended scaling is not important in binary mixtures until $\varepsilon > 10^{-2}$, whereas it is necessary for pure fluids (Estler, et.al., 1975; Hocken and Moldover, 1976) for $\varepsilon > 10^{-4}$. Our data corroborates this view. Since gravity effects

(Fannin and Knobler, 1974) and corrections to scaling (Greer, 1976) both cause the residuals to the coexistence curve fits to curve in the same direction (concave upward), care must be taken in analyzing the data to correctly explain its features.

This result for β is in very good agreement with recent Renormalization Group calculations (Kadanoff, et.al., 1976; Baker, et.al., 1976) for the Ising model and with recent measurements on pure fluids (Hocken and Moldover, 1976) and binary mixtures (Balzarini, 1974; Greer, 1976). These results provide evidence that pure fluids and binary mixtures belong to the same universality class as the Ising (lattice-gas) model. This is particularly important since it allows the results of binary mixtures, where gravity effects are generally smaller and corrections to scaling do not appear until very far from the transition, to be compared to Ising model predictions.

Thick Film Measurements

Now that the coexistence curve and the critical exponent β have been determined for the bulk system, showing Ising behavior, a thick film can be formed and analyzed to determine any deviations from bulk effects. In particular, a critical temperature dependence on spacing and any change in the critical exponents can be looked for. In order to investigate this behavior, the critical concentration of fluids was sealed in the variable spacing Fabry-Perot discussed earlier. This instrument has large, optically flat, high-reflectance mirrors between which a well defined film can be captured. Although the mirrors were originally flat to $\lambda/100$ on

the coated side, the process of sealing them caused some distortion so they were flat to approximately $\lambda/20$ in this thick film experiment. The method of determining the spacing between the flats will be discussed and then the critical temperature and coexistence curve measurements will be presented.

Spacing Determination

Since high reflectance coatings were used on our mirrors, the resulting interference fringes were very sharp (Francon, 1966) and well-defined (the ratio of fringe width to fringe separation was about 1/100). As discussed earlier, with the mirrors tilted slightly, three or four vertical fringes were observed from the opposite side of the flats by a measuring telescope. The stage on which the telescope travels has a resolution of ± 2 μm out of a total travel of 10 cm. In this work, only about 2 cm of the excursion was needed to do the precise measurements on the fringes.

To determine the separation between the flats from measuring the fringes, one considers the mirrors at a slight wedge angle as shown in Figure 14 with fringes forming for the two wavelengths λ_1 and λ_2 when the separations are L_1, L_2, and L_3 between the mirrors. The fringes observed are shown in Figure 15 with separation y between λ_1 and λ_2 and x between the m^{th} and m + 1 order of λ_1. The fringes form when twice the optical path length is equal to an integral number of wavelengths:

$$L_1 = m_1\lambda_1/(2n_1)$$

$$L_2 = m_2\lambda_2/(2n_2)$$

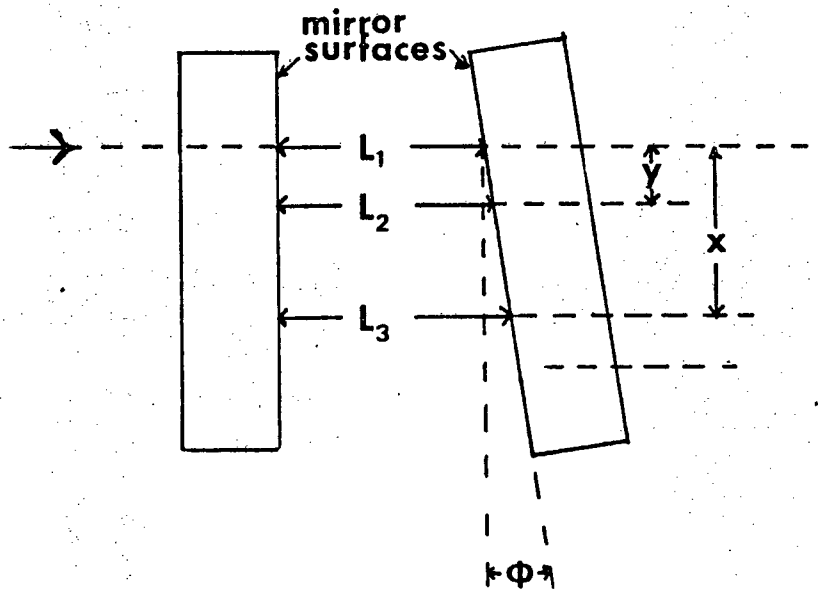

Figure 14: Side view of two flat mirrors tilted at an angle ϕ to the incident beam from the left. Constructive interference causes lines to be seen a distance y and x from the first line.

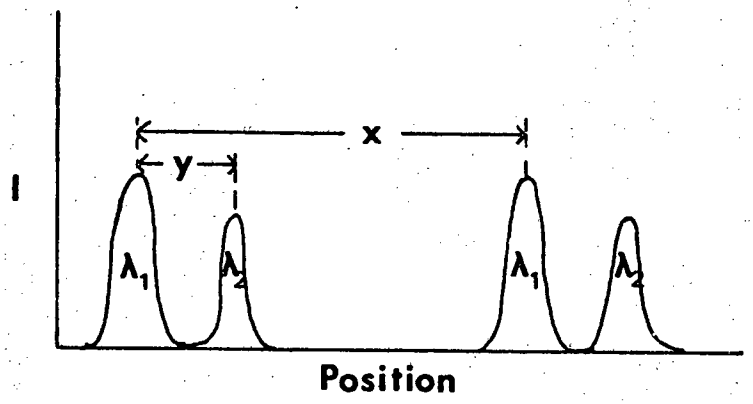

Figure 15: Intensity profile of lines seen through the telescope. y and x correspond to y and x in Figure 14.

$$L_3 = (m_1 + 1)\lambda_1/(2n_1).$$

Since the dispersion and temperature coefficient in the index of refraction is small (between 6328 Å and 5890 Å the dispersion is 0.1% and the temperature coefficient is $\sim$ 0.05%/K) we will let $n_1 = n_2 = n = 1.38$. The wedge angle, ϕ, is given by

$$\tan \phi = (L_2 - L_1)/y = (L_3 - L_1)/x$$

so that

$$(m_2\lambda_2 - m_1\lambda_1)/ny = \lambda_1/nx$$

In general, $m_2 = m_1 - m$ ($m = 0$ corresponds to being closer than the first coincidence) so that

$$L_1 = [m_2\lambda_2/\lambda_1 + y/x]\lambda_1^2/[2n(\lambda_2 - \lambda_1)] \qquad (\lambda_1 < \lambda_2)$$

is the spacing between the flats (see Figure 14). The spacing can be adjusted so that the fringes associated with the two wavelenges are at the same place (called coincidence with $y/x=0$) so that

$$L_c = m\lambda_1\lambda_2/[2n(\lambda_2 - \lambda_1)] \qquad \text{(at coincidence)}.$$

Some of the sources used in this experiment and the corresponding values of L_c are listed in Table III.

The initial spacing between the flats can be best determined by using two sets of doublets (such as the Hg and Na yellow doublets) and using the two resulting equations tc determine the two unknowns, L_1 and m. A problem arises because it is difficult to distinguish λ_1 and λ_2 for some sources such as the sodium yellow

TABLE III

LIGHT SOURCES USED IN THE THICK FILM CELL SPACING DETERMINATIONS AND THE CORRESPONDING FLAT SEPARATION FOR THE FIRST COINCIDENCE

Source	λ_1 (Å)	λ_2 (Å)	L_c (μm)	Filter used
H and He-Ne	6328	6566	6.3	6200 Å high-pass
Na and Hg	5770	5887	11	5780 Å band-pass
	5790	5893	12	
Hg	5770	5790	60	5780 Å band-pass
Na	5887	5893	209	5890 Å band-pass

doublet (although for Hg, $I(\lambda_2) \simeq 7\ I(\lambda_1)$); however, by knowing which way the wedge is oriented one can determine the initial spacing. After the initial spacing is determined all one does is count coincidences. (It is not quite this easy since when switching sources from say Hg yellow to H and He-Ne, one needs to know whether the ninth or tenth H and He-Ne coincidence (it is the ninth) corresponds to what one sees as the first Hg yellow coincidence--the only way to be sure is to squeeze down until the flats distort, which we did several times to check that a coincidence count was not lost in the opening and closing of the cell on the fluid.)

For all of the thick film data presented here, only the H and He-Ne lines were used to determine the spacing (although the others were used as an occasional check). In order to assure a uniform sample at the critical composition, the cell mirrors would be separated to 126 μm (twentieth coincidence) at a temperature about 0.7 K above the bulk critical temperature and the cell shaken approximately 800 times until the fringes were straight and uniform. The spacing would then be decreased until the desired separation was obtained. This sample could be used for smaller spacings but not for larger ones since the bulk fluid, which separates into two phases below T_c and mixes very slowly when above T_c, would be drawn between the flats. If the temperature was taken far below T_c for very small spacings, the separation would have decreased sufficiently (due to the cell's thermal expansion, ~ 0.65 μm/K) to allow bulk fluid of mostly one phase (due to the mirrors' position in the cell) to enter the sample when heated back toward T_c. For most

spacings at which data was taken, a new sample was prepared (the exceptions were 12 → 3 → 1 μm and 6 → 2.3 μm).

Since the effects in thick films were of interest, care was taken to avoid intrusion of the bulk fluids which surrounded the sample. Since most of the measurements were taken at or below the bulk critical temperature, the fluid surrounding the mirrors was mostly one phase (cyclohexane-rich) and any intrusion of this phase into the thick film sample was quite noticeable (see Figure 16). The time before such mixing occurred depended on the spacing; for the films of 30 μm and 60 μm it took about two days for noticeable mixing; for films of 6 μm and 12 μm it took about one week and for films 3 μm and smaller no mixing was ever observed (about two weeks). Once mixing had set in, no further measurements were attempted.

Determining the Critical Temperature

For each sample, with its known spacing, the critical temperature was measured. After the uniform sample had been captured by the method described in the previous sections, the temperature was lowered to about 20 mK above the expected value of T_c. The temperature was then lowered in steps until T_c was found. Then, an iteration procedure was used to determine the critical temperatures to ± 1 mK. The temperature steps were one and two mK, taking about a half hour for the system to come to equilibrium and with a three to five hour wait between steps.

Because of the high reflectance coatings on the mirrors, the resulting fringes were very sharp. The critical temperature for

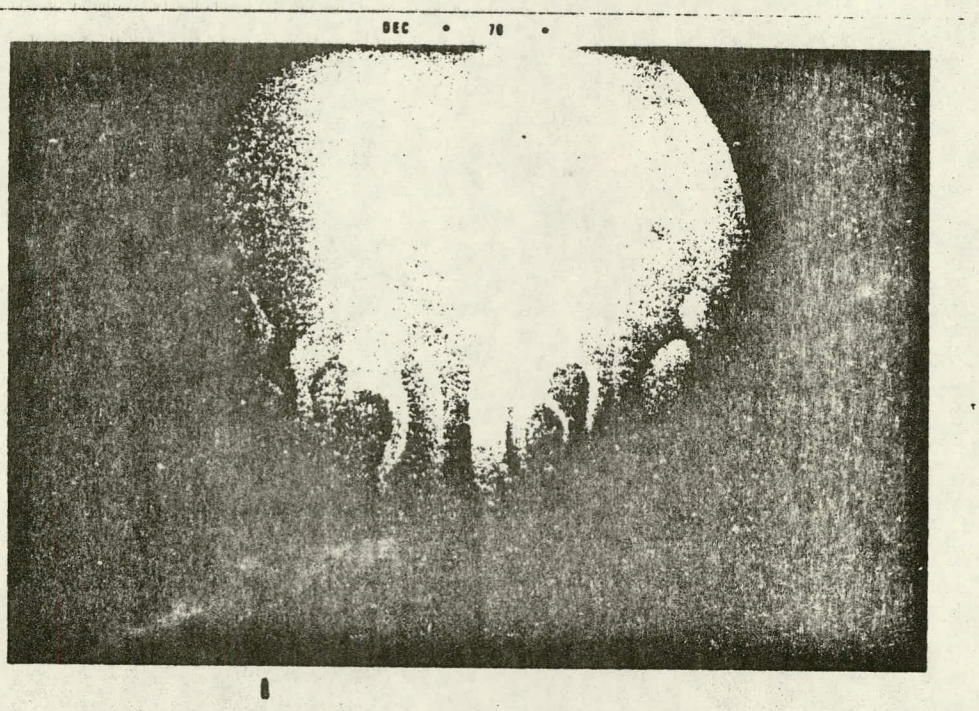

Figure 16: Photograph of the bulk fluid intruding into the thick film.

spacings larger than 12 μm was when this fine fringe would become broad and granular. The "granular" appearance of the fringes was attributed to the many drops which form between the flats on phase separation; however, the spacing was close enough (12 μm to 60 μm) that the extinction of the light did not occur. Otherwise, this transition was similar to that observed previously (Hartley, et.al., 1974) in a bulk (600 μm) system. However, when the spacing was 6 μm and smaller, the fringes split abruptly at the temperature that was associated with the critical temperature and did not display the graininess characteristic of larger spacings. Although surprised at first, we realized that the drops that form on phase separation were now large enough to span the space between the flats and so regions of each phase appeared as viewed through the telescope. Since each phase has a different refractive index, the differing optical path length causes the fringe to form in a different location and so "splitting" of the line is seen (see Figure 17). The regions of each phase (which I call "drops") were clearly seen when shining an unfiltered Hg lamp through the fluid since the broad blue-green bands that resulted allowed sufficient contrast to distinguish the drops. A picture of these drops is shown in Figure 18.

It is interesting to inspect the fringe splitting associated with these drops at this fairly large (6 μm) spacing (see Figure 19). In those regions where drops have formed, the lines have also split, but where no drops appear, the fringe does not split but becomes granular as in the lower left of Figure 18. It is felt that if the drops that form can span the space between the flats,

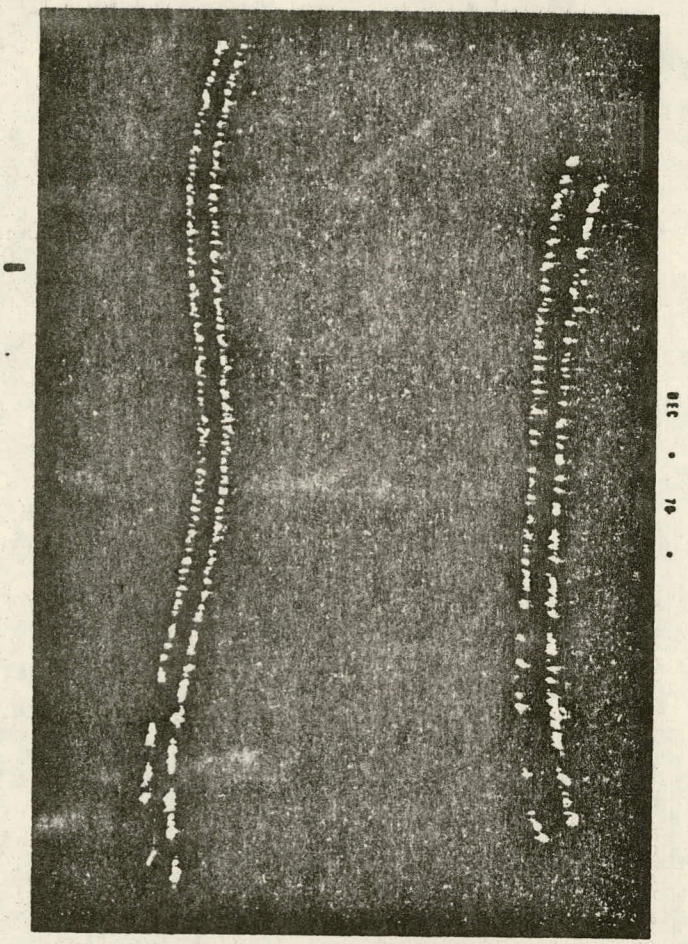

Figure 17: Photograph of the splitting of the fringe below T_c. This picture was taken of a film 1.6 μm thich and at a temperature of 44.585 C using a He-Ne laser light source.

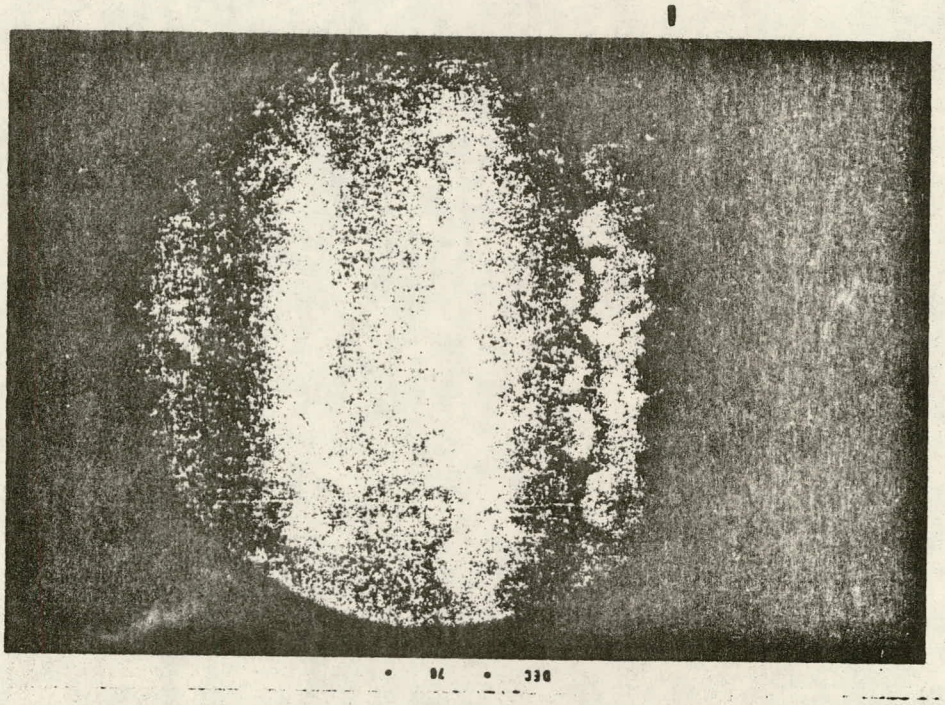

Figure 18: "Drops" spanning the flats as seen with an unfiltered Hg light source. The broad light bands are caused by the low reflectivity at these (blue-green) wavelengths. This picture was at L = 6 μm and $T_c(L) - T = 0.077°C$.

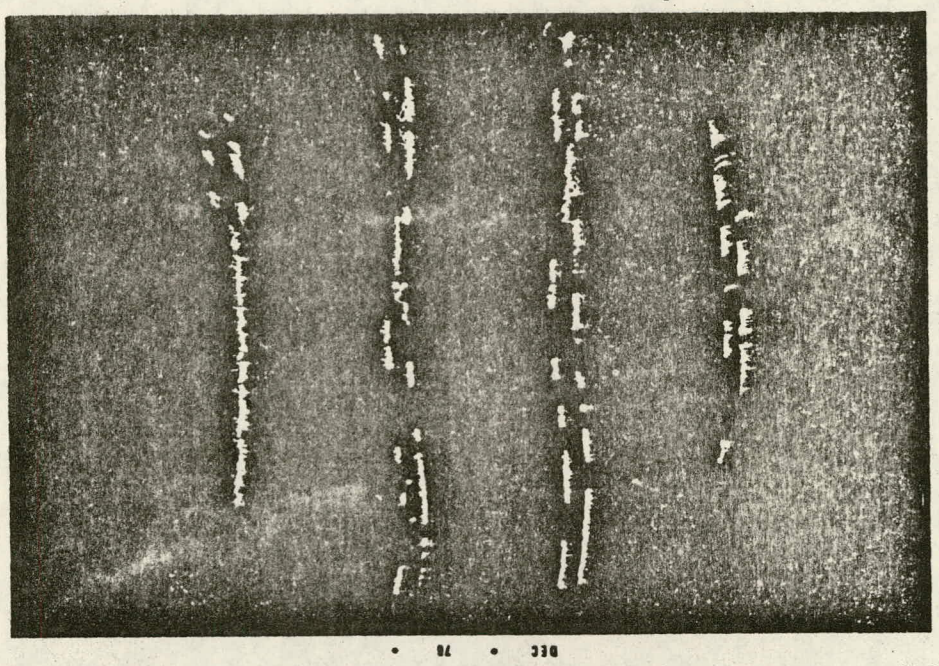

Figure 19: Photograph of the fringes associated with the drops in Figure 18 using a He-Ne laser light source.

as depicted in Figure 20a, then the fringes split. However, if the drops do not span the flats, as depicted in Figure 20b, then the fringes become "granular" for the reasons already discussed in connection with the larger spacings' critical temperature.

Since the fringe splitting is due to the difference in refractive index between the two phases, then by measuring the splitting we can determine the coexistence curve for these thick films. For the small (1 μm and 2 μm) spacings, the critical temperature could not be determined directly because of the resolution of the Fabry-Perot and the shape of the coexistence curve. A discussion of these points is done in the next section. The results of the critical temperature determination are presented in Table IV. As a point of reference, the critical temperature as determined from a bulk (800 μm) sample was found to be 0.5 ± 1.0 mK below the 60 μm critical temperature; however, if the cell was shaken so that the fluid in the surrounding reservoir could be examined, then its critical temperature was found to be 6 ± 1.0 mK below the critical temperature for 60 μm. At this large spacing the fringes became very broad and granular at the critical point. This shift in T_c from a bulk (800 μm) to the reservoir fluids (~2000 μm) is most probably due to a temperature gradient in the cell but could be due in part to a finite size effect. However, over the region of the flats, the temperature gradient, as determined by observing the appearance of the fringes at the critical temperature, was less than 2 mK.

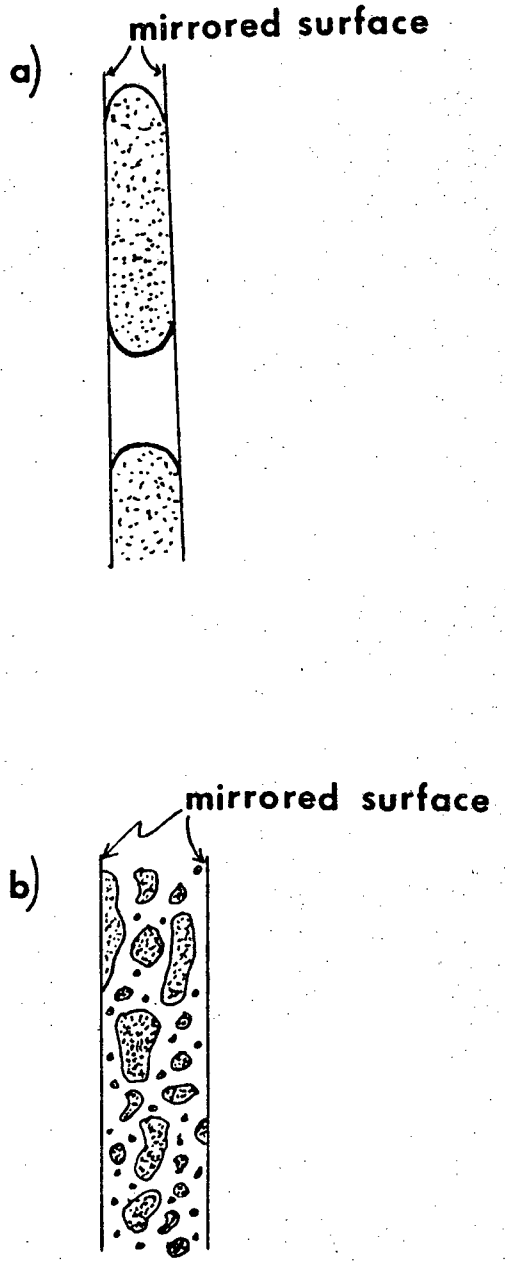

Figure 20: a) Drops spanning the space between the flats.

b) Drops not spanning the space between the flats.

TABLE IV

CRITICAL TEMPERATURE, $T_c(L)$, AS A FUNCTION OF SPACING, L

L (μm)		$T_c(L)$ (°C) (uncalibrated)
(bulk)	2000 (shaken)	45.517 ± 0.001
	800 (unshaken)	45.5225 ± 0.001
	60	45.523 ± 0.001
	32	45.525 ± 0.001
	13	45.528 ± 0.0007
	6	45.5305 ± 0.0015
	3	45.533 ± 0.001

Coexistence Curve for Various Spacings

When phase separation occurred, causing distinct regions between the flats at close spacing, the fringes split. A measurement of this splitting allowed the difference in refractive index between the two regions (phases) to be calculated. To see how this relation is obtained, we again consider Figures 14 and 15, where now, instead of a fringe being separated a distance, y, from the first due to the wavelength being different, the optical path length is different due to a different n. (It is assumed here that the drops span the space between the flats.) Then

$$L_1 = m_1\lambda_1/(2n_1)$$

$$L_2 = m_1\lambda_1/(2n_2)$$

$$L_3 = (m_1 + 1)\lambda_1/(2n_1)$$

so that

$$y/x = 2L_1n_1(n_1 - n_2)/(\lambda_1n_2).$$

Since $n_1 \simeq n_2 = n$ then

$$y/x = 2L_1\Delta n/\lambda_1,$$

so that the fringe shift, y, over the fringe spacing, x, is equal to twice the ratio of the flat spacing, L, to vacuum wavelength, λ_1, times the difference in refractive index between the two phases. As can be seen, the values of Δn accessible to experiment depend on the spacing, L, and the resolution of the instrument, (y/x). The smallest ratio of fringe splitting to spacing (y/x)

observable is related to the mirror's reflectivity, $r^2 = 0.99$, and the number of full widths, Γ, needed between the fringes before the split is visible. If we assume that one Γ between the fringes allows a visible separation, then

$$(y/x)_{min} = 2(1 - r^2)/r \simeq 0.013.$$

The coexistence curve data was determined from measurements of the fringe splitting and spacing using a traveling telescope, to a precision of ± 5 μm. Although the instrument is capable of ± 1 μm resolution, it was difficult to measure the broken fringes due to their curvature and fringe "pieces" not being adjacent (especially for thicker flat spacings). Due to this difficulty, photographs were taken of the fringe splittings to allow separate measurements with a microscope's reticle. Since the photograph could be oriented so the fringes were parallel to the reticle, an average fringe splitting could be determined over the length of the fringes. Also, for the very fine splittings (at the small spacings) only the photographs were usable in measuring the fringe split. The precision of measurement using the photographs was the same as with measurements from the traveling telescope.

The measurements were made as the temperature was raised and lowered; the data in Table V show the reproducibility of the measurements. After a temperature change was made and the system had attained thermal equilibrium, a measurement was taken. Occasionally, the measurement would be retaken after an additional period of time had elapsed; the two measurements agreed within experimental error. These coexistence curve data are presented in

TABLE V

THICK FILM COEXISTENCE CURVE DATA*

L (μm) (± 0.1 μm)	T (°C) (± 0.0001)	Δn	Measurement error on Δn
1.0	45.406 ↓	0.0041	± 0.0008
0.9	45.310 ↓	0.0060	± 0.0010
0.86	45.207 ↓	0.0078	± 0.0012
0.7	43.617 ↓	0.0086	+ 0.0020 - 0.0010
0.9 + 0.2 - 0.1	43.617 ↓	0,0131	+ 0.0024 - 0.0016
1.2 + 0.2 - 0.1	43.617 ↓	0.0157	+ 0.0022 - 0.0014
1.6	44.585 ↓	0.0141	± 0.0003
2.1	45.301 ↓	0.0095	± 0.0002
2.2	45.372 ↓	0.0080	± 0.0002
2.2	45.4234 ↓	0.0063	± 0.0004
2.2	45.4533 ↓	0.0054	± 0.0002
2.3	45.4841 ↓	0.0048	± 0.0002
2.3	45.4848 ↑	0.0042	± 0.0002
2.3	45.505 ↓	0.0030	± 0.0002
2.3	45.5155 ↑	0.0028	± 0.0003
2.3	45.5151 ↓	0.0028	± 0.0002
2.3	45.5255 ↑	0.0021	± 0.0004
3.0	45.527 ↑	0.0029	± 0.0003
3.0	45.523 ↓	0.0036	± 0.0002
3.0	45.505 ↑	0.0058	± 0.0002
3.0	45.469 ↑	0.0078	± 0.0002
3.0	45.418 ↓	0.0105	± 0.0002
5.9	45.501 ↓	0.0059	± 0.0002
5.9	45.465 ↓	0.0076	± 0.0002
5.9	45.521 ↑	0.0036	± 0.0002
5.9	45.526 ↑	0.0023	± 0.0002

*Coexistence curve measurements on thick films of spacing, L. T is the temperature with ↑ (↓) indicating the temperature was raised (lowered) in reaching T, and Δn is the difference in refractive index between the two phases.

Table V. The errors on Δn quoted in Table V include the error in measuring the fringe splitting and fringe spacing and the uncertainty in the flat separation, but not the uncertainty in the temperature or in $T_c(L) - T$. The data in Table V will be discussed after some theory is presented.

CHAPTER IV

SCALING THEORY IN THICK FILMS

Scaling theory has been introduced at the beginning of this work and was shown to give relations among the critical exponents which have been experimentally verified. Appendix A gives a "justification" of Scaling as a result of the system's invariance to a change of length (referred to as "Renormalization Group"). Group theory can give relations among quantities by investigating the geometry; however, actual numbers are calculable only when a specific model is used. Since a model describing the interaction of the walls with the fluid near a critical point has yet to be devised, only the geometry ("Scaling Theory") will be presented here, following the treatment given by Fisher (1971, 1973). However, the data will allow future models to be tested.

We will consider a system which is effectively infinite in two of its dimensions but of a finite thickness, $L = \ell\xi_0$, in a third dimension, where ξ_0 is the mean lattice or molecular size and ℓ is a dimensionless integer. If $L \simeq \xi_0$, then the system can be thought of as "two-dimensional" (neglecting wall forces). However, if $L >> \xi_0$, then one may expect a "crossover" from the three-dimensional to one characteristic of "two-dimensions" when $L \simeq \xi$, the correlation length of the system, so that the system is constrained from having fluctuations larger than L in one dimension.

The correlation length, ξ, is assumed to uniquely describe the size of the system's fluctuations and be given by a simple power law divergence $\xi = \xi_0[|T_c - T|/T_c]^{-\nu}$. The constant ξ_0 is ξ evaluated at $T = 0K$ and is identified with the mean molecular size and therefore is independent of temperature and spacing. For our binary fluid mixture, $\xi_0 \simeq 2.5$ Å.

The crossover from three- to two-dimensional behavior can be characterized by a crossover temperature, T_x, even though such a crossover may not take place abruptly. By our scaling assumption, such a crossover should occur when $L \simeq \xi$, which means

$$(1) \qquad [T_c(L) - T_x]/T_c(\infty) \equiv t_x \propto L^{-\theta}$$

where $\theta = 1/\nu$ if crossover occurs when $L \simeq \xi$. Notice that we have allowed the critical temperature to depend on the spacing, L.

To see how the critical temperature might depend on spacing, we will consider a heuristic argument. Let ℓ_1 be the size of a lattice in each of the two large dimensions in units of the lattice spacing, ξ_0. The bulk energy, E_∞, can be written as $E_\infty = \ell_1^2 \ell E_0$, where E_0 is the average energy per molecule in the bulk and the surface energy, E_s, as $E_s = (\ell_1^2 + 2\ell\ell_1)E_0^s$, where E_0^s is the average energy per molecule at the surface. The transition temperature goes as the energy--

$$\text{bulk:} \qquad kT_c(\infty) \propto E_\infty = \ell_1^2 \ell E_0$$

$$\text{constrained:} \quad kT_s \propto E_s + E_\infty = (\ell_1^2 + 2\ell_1\ell)E_0^s + \ell_1^2\ell E_0$$

so that

$$1 - T_s/T_c(\infty) = -(\ell_1^2 + 2\ell_1\ell)E_0^s/(\ell_1^2\ell E_0) \xrightarrow[\ell<<\ell_1]{} A/\ell, \quad A \equiv -E_0^s/E_0$$

or

$$[T_c(\infty) - T_c(\ell)]/T_c(\infty) = A/\ell, \qquad (T_c(\ell) \equiv T_s).$$

Model calculations can be carried out for different boundary conditions--for the Ising model the result of numerical approximations (Fisher, 1971) is

$$t_t \equiv [T_c(\infty) - T_c(\ell)]/T_c(\infty) = b/\ell^{\lambda} \tag{2}$$

with the sign and magnitude of b depending strongly on the boundary conditions and with $\lambda = 1$ for systems with a constraint (such as constant density or composition) and $\lambda = 1/\nu$ otherwise (e.g., constant pressure or chemical potential) (Fisher, 1973). These calculations are Ising-like in the sense that the nearest-neighbor interactions go over to nearest-"block" interactions. For a long range interaction (that is, infinite in extent), the critical region is independent of dimensionality ($\lambda \to 0$ (Fisher, 1971)), and the critical exponents (or the fixed point discussed in Appendix A) are constant.

Let us now consider a particular divergence as the spacing is varied. In order to make a comparison with the experiment, the shape of the coexistence curve, governed by the critical exponent β, will be analyzed:

$$\Delta\phi \simeq At^{\beta} \quad \text{as } T \to T_c(\infty)_- \tag{3}$$

where $t = [T_c(\infty) - T]/T_c(\infty)$ and $\Delta\phi$ is the change in volume fraction

which was shown in the preceeding chapter to be proportional to the difference in refractive index between the two phases. For small ℓ this becomes

$$\Delta\phi_\ell = A(\ell)\dot{t}^{\dot{\beta}} \quad \text{as } T \to T_c(L)_- \quad (\ell \text{ fixed}) \tag{4}$$

where $\dot{\beta} = \beta_{d-1}$ ($\beta_d = \beta$) and $\dot{t} = [T_c(\ell) - T]/T_c(\infty) = t - t_t$.

We make the scaling hypothesis that the only relevant variable affecting the crossover from (3) to (4) is $L/\xi \sim \ell t^\nu$. A convenient form to postulate (Fisher, 1971) is

$$\Delta\phi_\ell \simeq \ell^\omega X(\ell^\theta \dot{t}) \equiv \ell^\omega X(x), \quad (\theta = 1/\nu), \tag{5}$$

where the exponent ω is determined by matching (5) to (3) as $\ell \to \infty$. ($X(x)$ is the "shape function for the finite-ℓ critical behavior" (Fisher, 1971).) If we let $x \to \infty$ in (5) then bulk behavior must result so that

$$X(x) \simeq X_\infty x^\beta$$

or

$$X_\infty \ell^\omega \ell^{\theta\beta} t^\beta = A t^\beta$$

$$A = X_\infty \tag{6}$$

$$\omega = -\theta\beta.$$

We can also determine A_ℓ by examining (5) in the limit of small x where

$$X(x) \simeq X_0 x^{\dot{\beta}}$$

$$\Delta\phi_{\ell}(T) = \ell^{-\beta\theta} X_0 \ell^{\theta\dot{\beta}} \dot{t}^{\dot{\beta}} = A(\ell)\dot{t}^{\dot{\beta}}$$

$$A(\ell) = X_0 \ell^{\theta(\dot{\beta}-\beta)}. \tag{7}$$

This $A(\ell)$ will smoothly go over to A if $X_0 = A$ and $\dot{\beta}$ flows smoothly to β (as it does since it can be determined by an $\varepsilon = 4 - d(x)$ expansion) as $x \to \infty$. The prediction of $A(\ell)$ can be verified independently of β and $\dot{\beta}$. The relation of (5) represents a "law of corresponding states" such that if $\ln[L^{\theta\beta}\Delta\phi]$ is plotted versus $\ln[L^{\theta}\dot{t}]$ for different values of L, a universal curve given by $X(x)$ should result.

Scaling Theory can also provide some insight into the effects of the surfaces on the bulk behavior. Take the limit $\ell >> 1$ at fixed t; the coexistence curve should be described (Fisher, 1971) by

$$\Delta\phi_{\ell} \simeq \Delta\phi_{\infty} + 2\ell^{-1}\Delta\phi^{s} + \ldots \qquad (\ell \to \infty) \tag{8}$$

where the second term on the right is the surface correction to the bulk behavior. The first term is just the bulk critical phenomena which is being corrected by a term which will likely diverge at its own critical point, $T_c(L) \neq T_c(\infty)$. In fact, we have already argued that close to $T_c(L)$, or for small ℓ, that the coexistence curve should behave as in (4). Thus (8) should hold only away from the critical temperature shift or crossover. The scaling function defined by (5) can be generalized to

$$X(x) \simeq X_{\infty}x^{\beta} + Y_{\infty}x^{\phi}$$

where the first term is necessary to give the bulk behavior and the

second term is a postulated correction where ϕ will be determined. Thus

$$\Delta\phi_{\ell} \simeq X_{\infty}[t - t_t]^{\beta} + \ell^{\omega+\theta\phi}Y_{\infty}[t - t_t]^{\phi} + \ldots$$

which, when expanded and using (2) for t_t, gives (with $\omega = -\theta\beta$)

$$\Delta\phi_{\ell} \simeq At^{\beta} - A\beta b\ell^{-\lambda}t^{\beta-1} + Y_{\infty}\ell^{\theta(\phi-\beta)}t^{\phi} + \ldots \tag{9}$$

There are three cases to be considered when matching this equation to equation (8): $\lambda = 1/\nu > 1$, $\lambda = 1$ and $\lambda < 1$.

If $\lambda = 1/\nu > 1$, then the third term will dominate the second in equation (9) so that for an ℓ dependence as in (8), ϕ must be given by

$$\phi = \beta - \nu, \quad (\lambda = 1/\nu > 1)$$

so that $\Delta\phi^{s} \simeq A^{s}t^{\beta^{s}}$ with

$$A^{s} = Y_{\infty}/2 \quad \text{and} \quad \beta^{s} = \beta - \nu \quad (\lambda = 1/\nu > 1). \tag{10}$$

Thus the value of β^{s} is predicted from the (three dimensional) values of β and ν. Unfortunately, neither the sign nor magnitude of A^{s} is intimated.

The more applicable case for this work is when $\lambda = 1$, due to the constraint of constant density (composition) for the various film thicknesses (Fisher, 1971, 1974). Now the correction terms in (9) become

$$\Delta\phi^{s} = -A\beta bt^{\beta-1}/2 + Y_{\infty}t^{\beta-\nu}/2$$

but since $\nu < 1$, (at least in three dimensions) then the first

term dominates (since the exponent of t is less in the first than second term) allowing the important predictions

$$A^s = -\tfrac{1}{2}A\beta b \quad \text{and} \quad \beta^s = \beta - 1 \quad (\lambda = 1). \tag{11}$$

Thus, the first correction to the bulk behavior is completely predicted since A and β are known from bulk measurements and b is determined from the critical temperature dependence on spacing.

Finally, if $\lambda < 1$, then equation (8), which allowed a surface correction to the bulk behavior, breaks down. As Fisher (1971) has pointed out, $\lambda \to 0$ corresponds to long range ordering in the fluids in which case a separation of surface properties from bulk properties would not occur.

CHAPTER V

COMPARISON OF THEORY AND EXPERIMENT

Testing the Theory

We are now in a position to analyze our data and compare it with the theory just presented. The critical temperature shift from the bulk (unshaken, 800 μm) value is plotted in Figure 21 as a function of spacing, L, from the data in Table IV. This plot shows that a logarithmic dependence of $T_c(L) - T_c(\text{"}\infty\text{"})$ on L fits the data very well. The best fit to the data with an L^{-1} dependence is also shown in Figure 21 not to be inconsistent with the data but not to fit it as well. The explanation of the apparent logarithmic dependence will be postponed until the coexistence curve data are analyzed and a connection between the two sets is made.

It was shown at the end of Chapter III that the difference in refractive index, Δn, between the two phases can be determined by measuring the ratio of the fringe shift, y, to the fringe spacing, x, and the spacing, L:

$$\Delta n = (\lambda_1/2L)(y/x).$$

Further it was shown that the resolution of the optics provided a minimum measurable value of $y/x \simeq 0.013$. This results in a minimum value of Δn that depends on the spacing, L. This inaccessible region is the lower left triangle in Figure 22 with the solid line

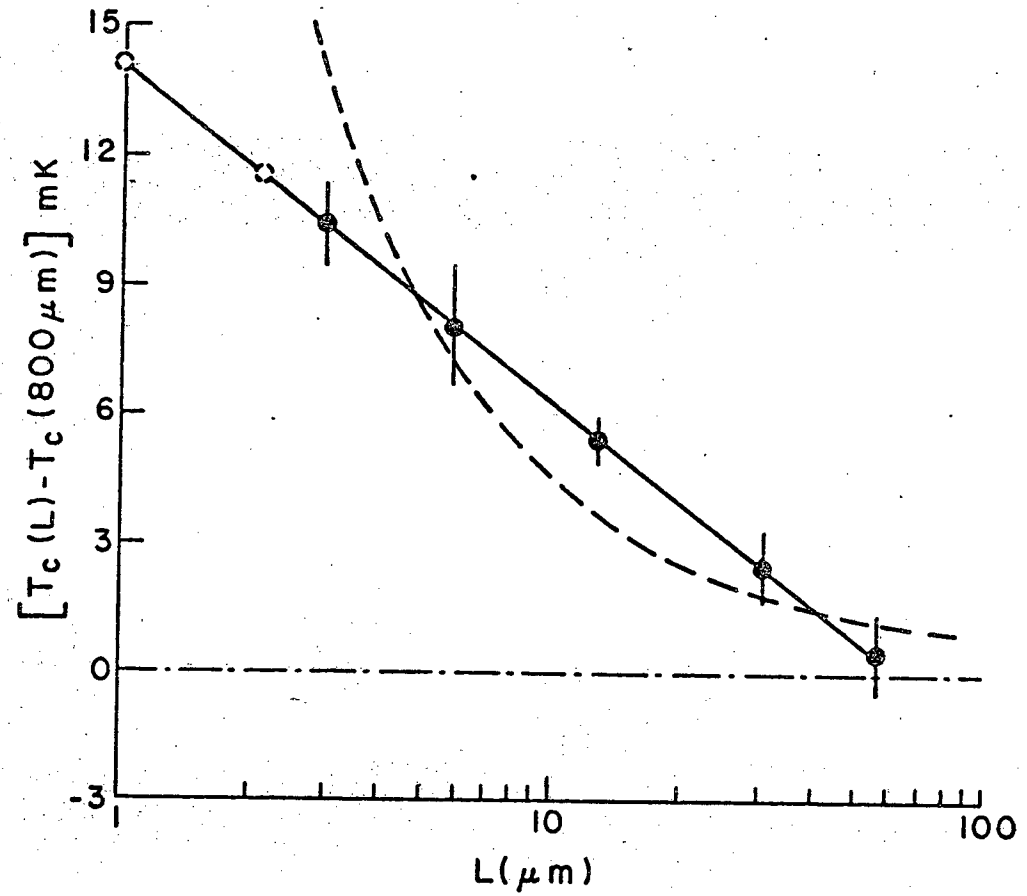

Figure 21: Shift in critical temperature relative to the bulk (800 μm) value as a function of flat spacing, L. The solid line is a fit to a log (L) dependence; the dashed line is the best fit to the data for L^{-1} dependence. The dashed circles are the extrapolated values of $T_c(L)$ used for the coexistence curve.

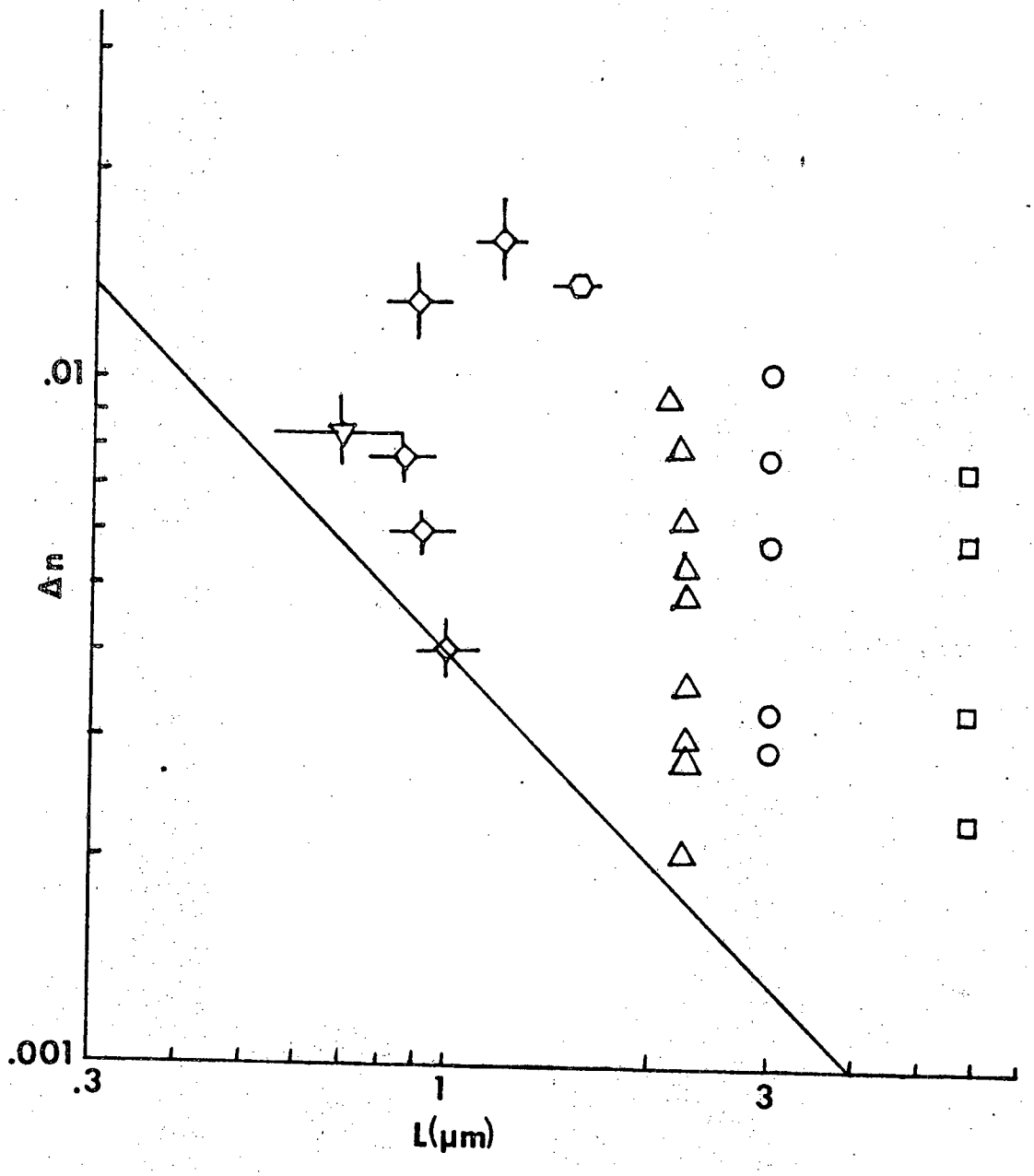

Figure 22: Accessible region and the coexistence curve data that was taken with our optical system. For the region below the solid slanted line, the fringe splitting cannot be resolved with our 99% reflective mirrors. The symbols used are the same as in Figure 23.

being the theoretical lower limit of experimentally observable data. Also plotted in Figure 22 are the data that were taken in the thick film coexistence curve experiment and listed in Table V. It can be noted that data was taken as close to the resolving limit of the "Fabry-Perot" interferometer as possible, (particularly at small spacings). Thus, the critical temperature, as determined by the "drops" forming or the lines splitting, could not be observed for small flat separations (< 3 μm)! It is only after the temperature is well below critical that the splitting can be resolved at these small flat spacings.

Critical temperatures for these spacings can be estimated either by extrapolating the $T_c(L)$ data in Figure 21, or by constraining the data points from Table V (and shown in Figure 23) to fit a straight line. We find the values of $T_c(L)$ obtained by extrapolating the logarithmic curve in Figure 21 to be the values obtained by fitting the coexistence curve data shown in Figure 23 within experimental error.

The coexistence curve data in Figure 23 are presented using the values of $T_c(L)$ from the logarithmic curve in Figure 21. These data were reproducible whether raising or lowering the temperature as shown in Figure 23. The results of the bulk coexistence curve are used to suggest the coexistence curve for thick films is again described by $\Delta n = A(L)\dot{t}^{\dot{\beta}}$ where $\dot{\beta}$ is perhaps a different value of β and $\dot{t} \equiv [T_c(L) - T]/T_c(\infty)$ (see equation (4) in Chapter IV). This form uses the critical temperature as a function of the spacing, L, determined (independently for 3 μm and 6 μm) from Figure 21. Thus, a plot of log Δn versus log $(T_c(L) - T)$ for the various flat

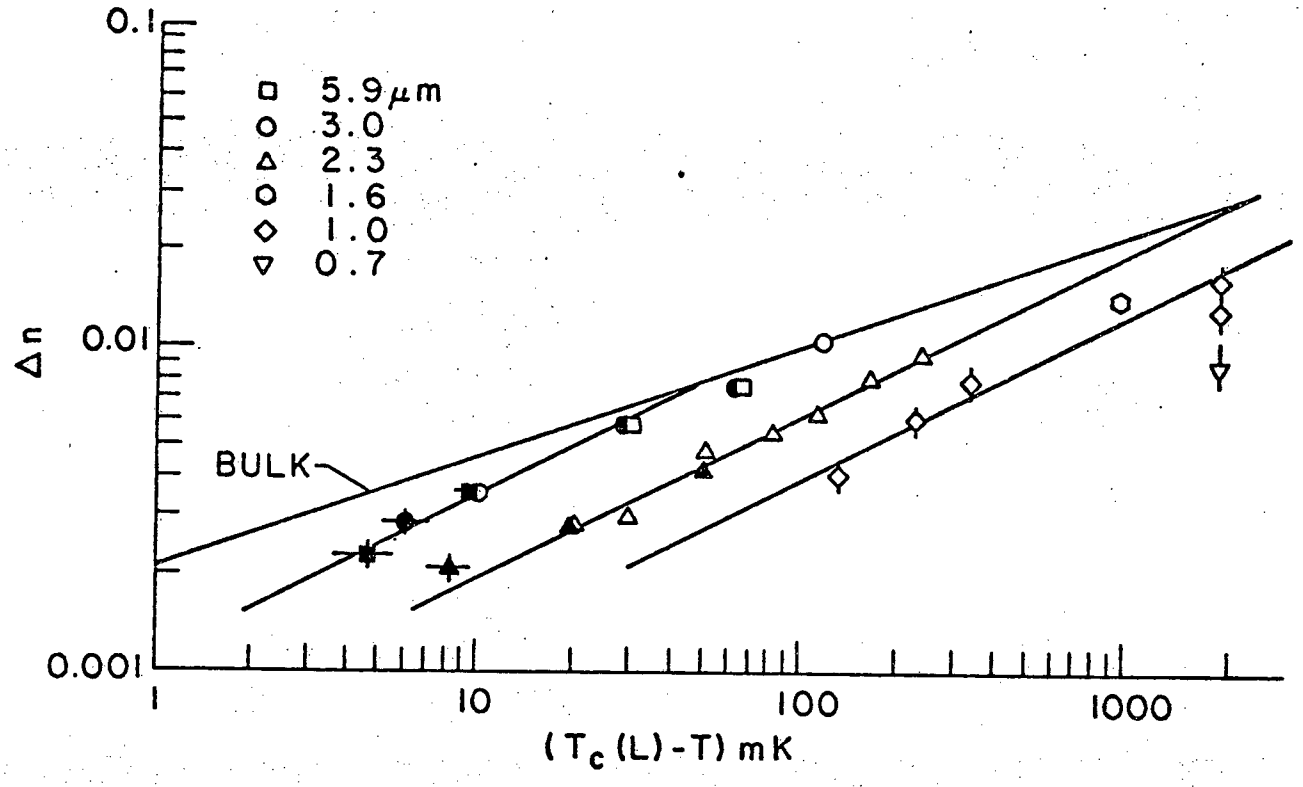

Figure 23: Coexistence curves for the various spacings. The bulk line is from Figure 13, and has a slope (β_3) of 0.326; lines drawn through the points have a slope (β_2) of 0.5. Open symbols are points taken while lowering (and solid symbols while raising) the temperature.

spacings should give a set of straight lines. A log-log plot of the data points does indeed appear to give a set of reasonably straight lines, for each flat spacing (see Figure 23). Since the most extensive of the coexistence curve data were obtained for a flat spacing of 2.3 μm (other than the large amount of data for the bulk fluid), a fit was made to determine the slope of a straight line through these data points. This slope is the critical exponent β and a weighted least squares fit gave $\beta = 0.49$ (with a standard deviation of $\pm$ 0.02) with a reduced chi square of 1.1. Straight lines with slope 0.5 were also drawn through the data points for the spacings 6 μm, 3 μm and 1 μm. These straight lines also suggest that $\beta \simeq 0.5$ for these spacings as well. It is interesting to note that coexistence curve data Hartley (1974) took at a flat spacing of 125 μm fall on the bulk curve. The bulk curve is the fitted line to the coexistence curve data taken with the prism cell as discussed previously.

An apparent "crossover" from bulk to "two-dimensional" behavior occurs in the 3 μm and 6 μm points and is also suggested in the 2.3 μm and 1.0 μm points. The strong dependence of the coexistence curve (or fringe splitting) on L is vividly shown in Figure 24, where L varies from $\sim$ 0.7 μm at the left fringe to $\sim$ 1.2 μm at the right one, but where the fringe splittings differ by more than a factor of two. Since the critical temperature seems to vary so slowly with spacing (see Figure 21), then these three fringes give values of Δn at effectively the same value of $T_c(L) - T$, ($\simeq$ 2 K, and are the three points at the right in Figure 23) and show the large dependence on spacing of the amplitude, A(L).

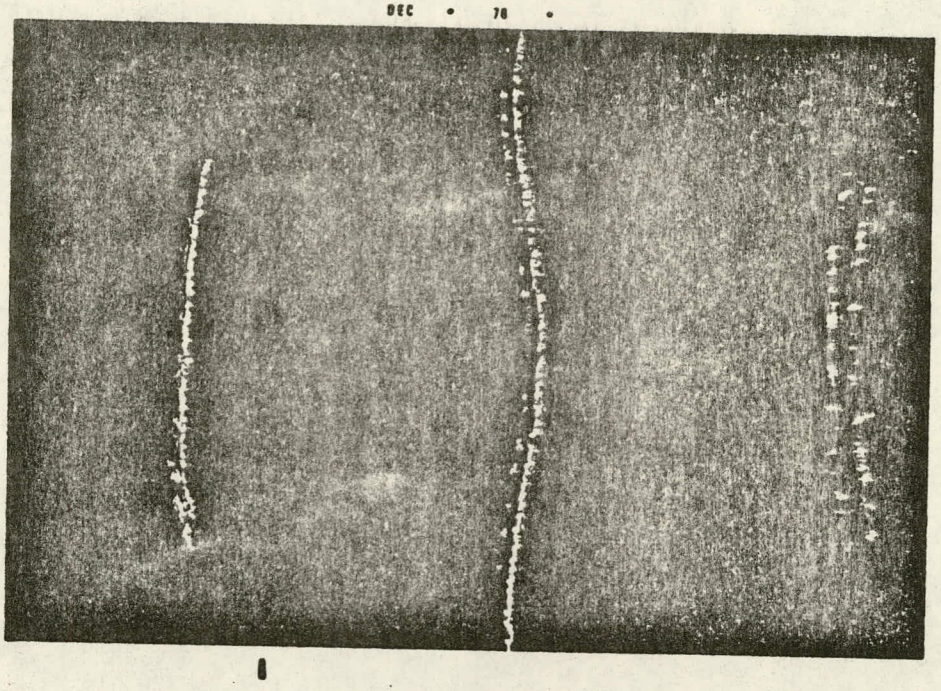

Figure 24: Photograph of fringe splittings almost 2°C below the critical temperature using a He-Ne laser light source. Flat separation at the center fringes is 0.9 ± 0.1 μm and the fringes on the left (right) are at a separation $\lambda/2n$ smaller (larger) than at the center. The fringe splitting is barely detectable at the left but is quite large at the right--much more so than the factor of two difference in spacing would allow. These three points are the highest $T_c(L) - T$ points shown in Figure 23.

Our value for $\beta = 1/2$ is the mean field (infinite range) value and agrees with the experimental results of Hawkins and Benedek (1974) and Kim and Cannell (1976) on monomolecular films on water, which should simulate a two-dimensional liquid-gas transition in the absence of wall forces. The mean field value for β is consistent with the apparent logarithmic dependence of the critical temperature on spacing (Figure 21). The scaling arguments presented in the preceeding chapter predict that $T_c(L)$ should behave as $L^{-\lambda}$, with $\lambda = 1$ when the fluid composition is constant for various spacings (Fisher, 1971). However, Fisher (1971) has stated that for long range interactions, λ approaches zero, which results in either no dependence of $T_c(L)$ upon spacing or the logarithmic dependence which seems to (best) fit our data.

Although the logarithmic curve fits the data in Figure 21 from $L = 1$ to 60 μm very well, we cannot extrapolate this dependence to larger spacings. Whether the logarithmic dependence is followed at larger spacings is a crucial question since the geometry of even "bulk" cells would then be very important. Our result indicates that for every decade change in spacing the critical temperature should change by ~ 7.7 mK--not a huge effect but certainly one that could be seen if looked for. The 800 μm (bulk, unshaken) critical temperature (see Table IV) indicates that the logarithmic dependence does not contiue to this large a spacing. However, the discrepancy noted earlier between the shaken and unshaken critical temperatures at 800 μm flat spacing could be explained as a finite size effect.

The amplitude dependence of Figure 23 is very interesting since it allows the determination of θ and the general scaling function $X(x)$ (see (7) and (5) in Chapter IV). If, for all the spacings shown in Figure 23, the value of $\beta = 0.5$ is used (which fits the data quite well) then the amplitude dependence on spacing can be plotted as in Figure 25. The Scaling Theory presented in Chapter IV predicted (equation (7)) that $A(L) \propto L^z$ where $z = (\dot{\beta} - \beta)\theta = (\dot{\beta} - \beta)/\nu$. Using our measured value of $\dot{\beta} \simeq 0.5$ and $\beta \simeq 0.326$ and the three dimensional value for ν (0.64) then the Scaling Theory prediction for z is 0.27. However, our inferred amplitude dependence, shown in Figure 25, gives z in the range 0.6 to 0.8! The Scaling Theory prediction of $z = 0.27$ is shown in Figure 25 to be inconsistent with the amplitude dependence observed in this experiment. The fitted value of $z = 0.7 \pm 0.1$ gives $\theta = 4 \pm 0.5$ or, using the Scaling Theory assumption that "crossover" occurs when $\xi \sim L$, $\nu \sim 1/4$.

This discrepancy between the Scaling Theory prediction and this observation should not be too distressing. As Bergman, Imry and Deutscher (1973) point out, there are several assumptions that go into the predicted value of z, but the significant point is that there is a simple power law dependence of the amplitude on spacing. In fact, one can "patch up" the Scaling Theory given in Chapter IV by changing the scaling assumption that crossover occurs when $L \sim \xi$ to $L^2 \sim \xi$. This gives a value of $z = 4$ if $\nu = 0.5$ (the mean field value). Alternatively, one can merely not make the assumption that $\theta = 1/\nu$ so that the experiment determines the value of θ. (It should be noted that θ is the power law dependence of the crossover

Figure 25: Amplitude dependence on spacing. The dashed line is the predicted slope using Scaling Theory.

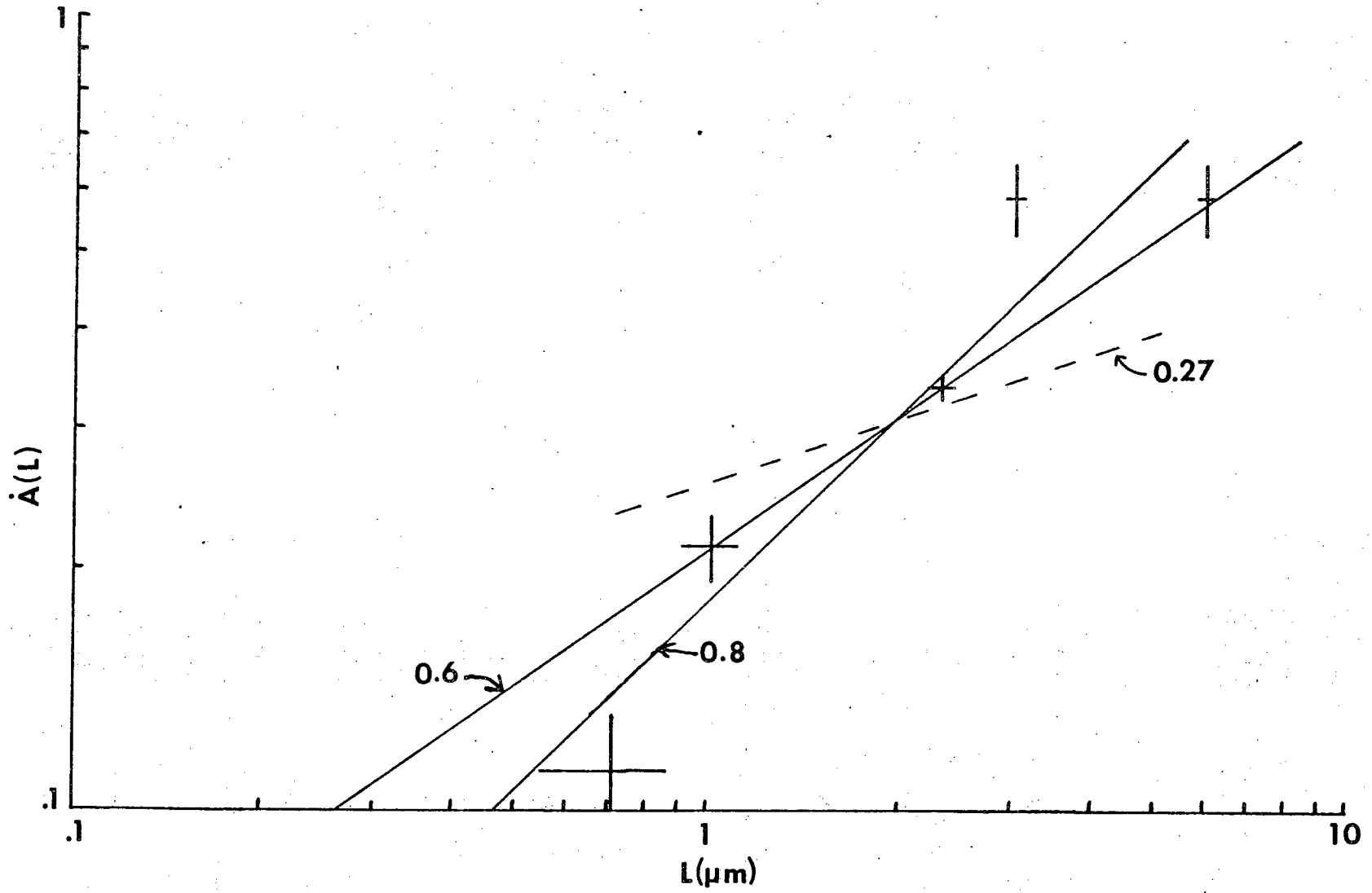
1
.1
.1
1
10
L(μm)
Ȧ(L)
0.6
0.8
0.27

temperature, t_x, given in equation (1) of Chapter IV. One can either calculate the crossover temperatures from extrapolating the lines in Figure 23 or determine the amplitudes (as has been done above). The amplitudes were chosen since they more accurately reflect the data in Figure 23 and are less dependent on the behavior near the actual crossover. However, in the formalism developed in Chapter IV, the two approaches are equivalent.)

The approach that is taken here is that θ is experimentally determined and not necessarily given by $\theta = 1/\nu$. This raises the question as to whether the Scaling theory predicts any special relationship between the data once the values of β, $\dot{\beta}$ and θ are determined. The answer is yes, indeed. The scaling function $X(x)$ defined in Chapter IV:

$$\Delta\phi_{\ell} = \ell^{-\theta\beta} X(\ell^{\theta}\dot{t}) \tag{5}$$

allows one to predict a universal curve given by $X(x)$ for all thick film data. Since $\ell^{\theta\beta}\Delta\phi_{\ell} = X(\ell^{\theta}\dot{t})$ then a log-log plot of $L^{\theta\beta}\Delta\phi_{\ell}$ versus $L^{\theta}\dot{t}$ should give a universal curve for all the data (Fisher, 1973). Such a curve is plotted in Figure 26 from the data in Table V using $\beta = 0.326$ and $\theta = 4$. The points fall on a curve that is fairly linear and independent of spacing. The circles lie "off" this curve presumably for the same reason they overlap the 5.9 μm data points in Figure 23.

If the correction due to the surfaces on the bulk behavior is attempted (using the Scaling Theory developed in the previous chapter) then one needs to assume that the critical temperature dependence on spacing can be described by L^{-1}. As described in the

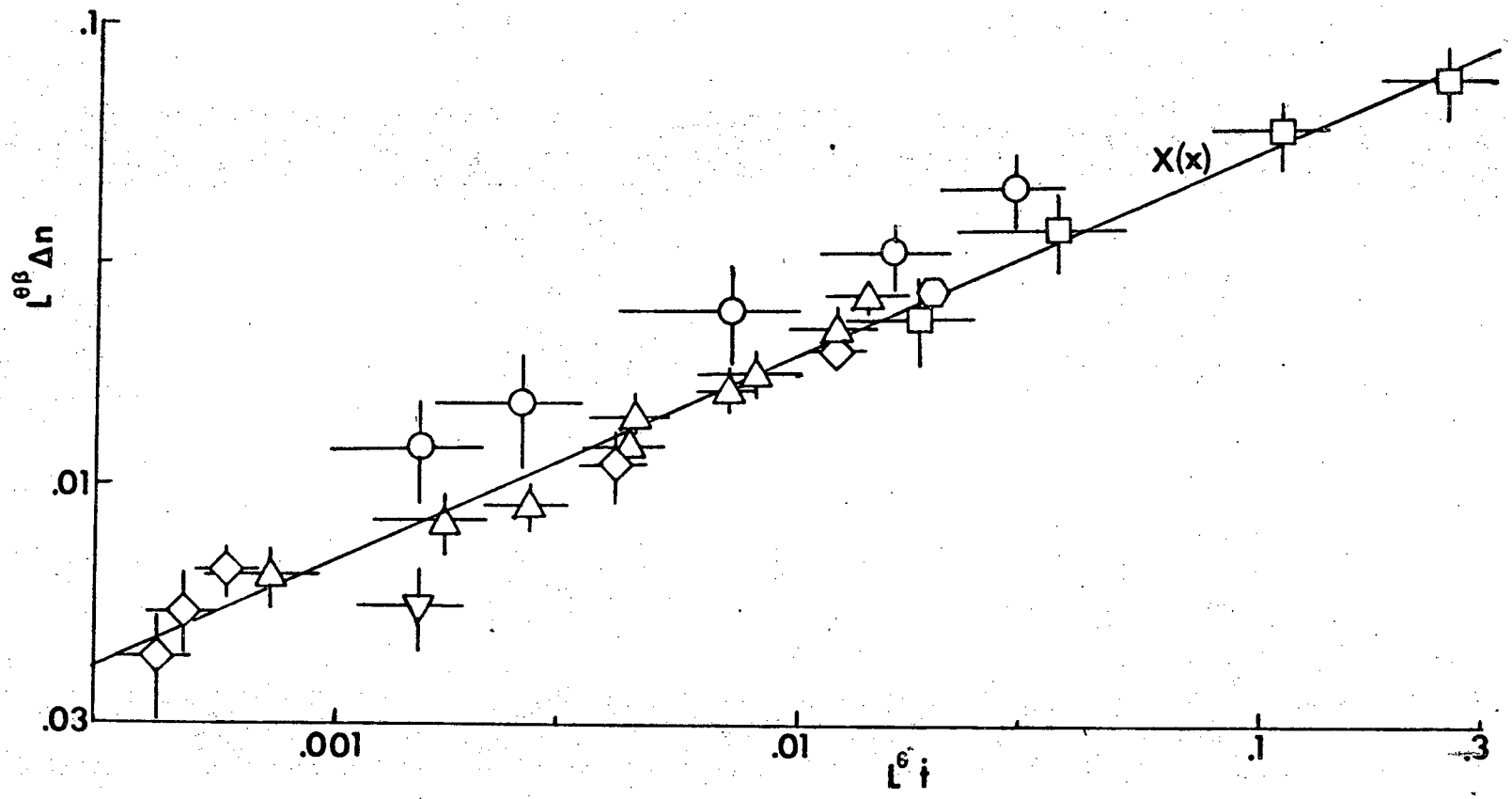

Figure 26: Scaling function X(x) is sketched (using $\theta = 4$ and $\beta = 0.326$) as a universal curve for all the data in Table V. The symbols are the same as those used in Figure 23. The error bars are larger at larger spacings, L, due to the uncertainty of θ which is the exponent of L. The slope of the line is 0.45 (L has units of μm).

previous Scaling Theory section, the surface correction is completely predicted (see equation (11)) knowing A (0.143) and β (0.326) from the bulk coexistence curve measurements and b (0.50) from the L^{-1} fit shown in Figure 21. If this correction term is used with the bulk term then the predicted effect is opposite to that observed experimentally as shown in the dot-dashed line in Figure 27. Should it be argued that the critical temperature dependence on spacing in Figure 21 could be $L^{-\lambda}$ with $\lambda = 1/\nu \gtrsim 1$ then the correction term is no longer completely specified but, in particular, may have the opposite sign. If the Y_∞ in equation (10) is taken to be $-A\beta b$ and $\lambda \gtrsim 1$ then the set of dashed lines in Figure 27 are predicted. As can be seen, the qualitative behavior of the surface correction term does not approximate the behavior of the data. (Note that the data are plotted versus $(T_c(\infty) - T)$ instead of $(T_c(L) - T)$ as was done in Figure 23.) This result is expected from the apparent long range behavior inferred previously, since the surfaces could not act independently of the bulk ($\lambda < 1$).

Since the long range behavior has been effectively shown, then a comment is necessary as to whether the long range behavior can be used to explain the low value for ν ($\sim 1/4$) that the data and Scaling Theory seemed to indicate. Fisher, Ma and Nickel (1972) have used Renormalization Group expansions to investigate long range interactions (as with dipole-dipole interactions) decaying in d dimensions as $\phi(r) \sim r^{-(d+\sigma)}$. This leads to classical values of the critical exponents $\beta \simeq (d/\sigma - 1)/2$ and $\nu \simeq 1/\sigma$, if $\sigma > d/2$. Using our experimental value of $\beta \simeq 1/2$ and if $d \sim 2$ then $\sigma \sim 1$ and so $\nu \sim 1$ which is not consistent with the Scaling Theory analysis

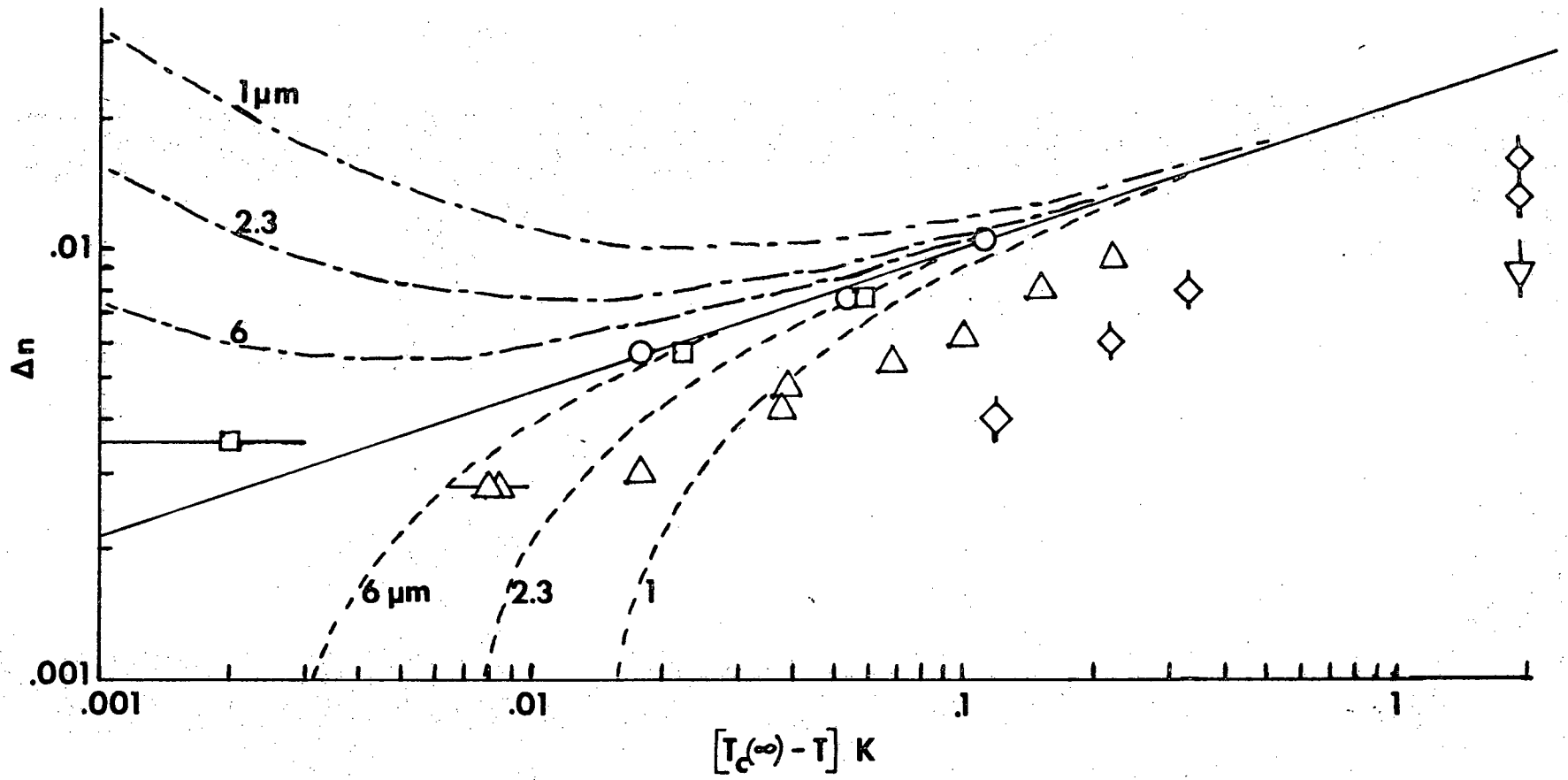

Figure 27: Surface corrections predict the dot-dash curves if $\lambda = 1$ and qualitatively predict the dashed curves if $\lambda \gtrsim 1$. The solid line is the bulk coexistence curve from Figure 11. The symbols for the data correspond to those used in Figure 23. Note that the "crossover" temperatures predicted do not agree with those observed experimentally (see also Figure 23).

of the amplitude dependence discussed previously where $\nu \sim 1/4$. In this case, Fisher's result duplicates the Ising model calculation for the critical exponents β and ν in two dimensions, and does not seem to clarify the value of ν the data suggests. It is interesting to note, however, that the dimensionality, d*, at which classical values of the exponents are observed is d* = 2 when long range ordering predominates. (As discussed in Appendix A, d* = 4 for short range interactions, e.g., the Ising model.)

Conclusions and Recommendations

This thesis has presented the first experimental data of the behavior of a critical system as it approaches two dimensionality. Evidence in the form of the bulk coexistence curve data and the resulting value of the critical exponent β has been presented to confirm predictions that a binary fluid mixture near its critical point is an Ising class system. This same binary fluid mixture was then constrained between two optically flat pieces of quartz so that the critical temperature and coexistence curve could be determined as the spacing between the flats was varied from 1 μm to 60 μm. The critical temperature was directly measured for spacings between 3 and 60 μm. It was found that if the walls were close enough together ($\lesssim$ 6 μm) then the drops that formed on phase separation would span the intervening space. The coexistence curves of these thick films was then determined from measurements of the difference in refractive index between the two phases that appeared as drops.

The theory concerning the behavior of the coexistence curve as a function of spacing was presented and then compared to our data. The theory accommodated the data very well but did not give the critical exponents that are expected from the exact two-dimensional Ising model, but rather gave a "mean field" value of $\beta \simeq 0.5$ that agreed with experimental results on a system which might be expected to simulate a two-dimensional lattice-gas (Ising model) transition. The critical exponent ν seemed to have a value near 1/4 (assuming the system "crosses over" when $L \sim \xi$), which has not been predicted for any model thus far.

The thick film data on the critical temperature dependence on spacing was shown to agree with the (largely) independent measurements of the coexistence curve dependence. These measurements suggested that long-range interactions were present in the fluids near the critical point. The crossover from normal three-dimensional behavior to the long range behavior was accommodated nicely by the existing Scaling Theory.

Clearly, more data is needed to determine whether the long range ordering observed here is typical of binary fluid (lattice-gas) transitions near two dimensionality (particularly with regard to having a polar component such as methanol, that might cause long range ordering for the binary mixture). The reason the critical exponent values were quite distinct from the predictions may lie in the interaction of the walls with the fluid. Since only one component (methanol) of the binary mixture is very polar, it is not clear to what extent a dipole-dipole type interaction with the walls will affect the critical behavior of the mixture. It would be

interesting to see if the amplitude dependence for other binary mixtures on spacing is as strong as indicated here.

I would suggest that similar measurements be attempted on a non-polar binary mixture to determine the importance of the wall-fluid forces. Additional experiments on different polar and nonpolar fluid mixtures would give additional details of this unknown interaction. Also, more extensive measurements on the critical temperature dependence on spacing should be conducted to determine if the dependence is logarithmic out to large spacings ("bulk" systems) or if it falls off faster (or "oscillates").

The implications of this research are far reaching and important for all aspects of critical phenomena. The effects on a critical system due to its finite size had not been measured in Ising class systems prior to this work. Should the logarithmic dependence of the critical temperature on film thickness be found to hold for "bulk" ($\sim$ 1 cm) systems as it did for our films ($3 < L < 60$ μm) then no system would be free of size effects. Our work suggests that the critical temperature decreases $\sim$ 8 mK for every decade increase in spacing. It is also important to realize that both this work and that on monomolecular films (Hawkins and Benedek, 1974; Kim and Cannell, 1976), both of which are expected to be lattice-gas transitions, gave a "mean field" value for the critical exponent, β. This may indicate that real critical systems have mean field exponents at and near two dimensions.

BIBLIOGRAPHY

B.J. Ackerson, C.M. Sorensen, R.C. Mockler, and W.J. O'Sullivan, Phys. Rev. Lett. 34, 1371 (1975).

Y.P. Bagoi, V.I. Sokhan and L.A. Pavlichenko, JETP Lett. 11, 190 (1970).

C.S. Bak and W.I. Goldburg, Phys. Rev. Lett. 23, 1218 (1969).

C.S. Bak, W.I. Goldburg, and P.N. Pusey, Phys. Rev. Lett. 25, 1420 (1970).

G.A. Baker, Jr., B.N. Nickel, M.S. Green, and D.I. Meiron, to be published.

D.A. Balzarini, Can. J. Phys. 52, 499 (1974).

D.J. Bergman, Y. Imry, G. Deutscher, and S. Alexander, J. Vac. Sci. Technol. 10, 674 (1973).

D. Bedeaux and P. Mazur, Physica 67, 23 (1973).

P.R. Bevington, Data Reduction and Error Analysis for the Physical Sciences (mcGraw-Hill, New York, 1969).

R.J. Birgeneau, H.J. Guggenheim, G. Shirane, Phys Rev. B1, 2211 (1970).

D.F. Brewer, J. Low Temp. Phys. 3, 205 (1970).

R. Brout, Phase Transitions (Benjamin, New York, 1965).

A.N. Campbell and E.M. Kartzmark, Can. J. Chem. 45, 2433 (1967).

C. Domb in Phase Transitions and Critical Phenomena, edited by C. Domb and M.S. Green (Academic, New York, 1974), Vol. 3, p. 433.

E.L. Eckfeldt and W.W. Lucasse, J. Phys. Chem. 47, 164 (1943).

W.T. Estler, R. Hocken, T. Charlton and L.R. Wilcox, Phys. Rev. A12, 2118 (1975).

A.A. Fannin, Jr. and C.M. Knobler, Chem. Phys. Lett. 25, 92 (1974).

M.E. Fisher, Reports on Progress in Physics, XXX, 615 (1967).

_____, in Critical Phenomena: Proceeding of the International School of Physics, "Enrico Fermi", Varenna, 1970, No. 51, edited by M.S. Green (Academic, New York, 1971), p.1.

_____, J. Vac. Sci. Technol., 10, 665 (1973).

_____, Rev. Mod. Phys. 46, 597 (1974).

M.E. Fisher, S.K. Ma, and B.G. Nickel, Phys. Rev. Lett. 29, 917 (1972).

M.E. Fisher and P.E. Scesney, Phys. Rev. A2, 825 (1970).

M. Francon, Optical Interferometry (Academic Press, New York, 1966).

M. Giglio and A. Vendramini, Phys. Rev. Lett. 35, 168 (1975).

G.H. Gilmer, W. Gilmore, J. Huang, and W.W. Webb, Phys. Rev. Lett. 14, 491 (1965).

M. Givon, I. Pilah, and U. Efron, Phys. Lett. 48A, 1 (1974).

W.I. Goldburg and P.N. Pusey, J. Phys. (Paris) Suppl. 33, C1, 105 (1972).

E.S.R. Gopal, R. Ramachendra, P. Chandra Sekhar, K. Govindarajun and S.V. Subramanyam, Phys. Rev. Lett. 32, 284 (1974).

M.S. Green, M.J. Cooper, and J.M.H. Levelt Sengers, Phys. Rev. Lett. 26, 492 (1971).

S.C. Greer, (to be published in Phys. Rev. A)

S.C. Greer, T.E. Block, and C.M. Knobler, Phys. Rev. Lett. 34, 250 (1975).

R. Griffiths, Phys. Rev. Lett. 24, 1479 (1970).

E. Guyon, J. Vac. Sci. Technol. 10, 681 (1973).

C.L. Hartley, Ph.D. Thesis, Univ. of Colorado (1974, unpublished).

C.L. Hartley, D.T. Jacobs, R.C. Mockler, and W.J. O'Sullivan, Phys. Rev. Lett. 33, 1129 (1974).

G.A. Hawkins and G.B. Benedek, Phys. Rev. Lett. 32, 524 (1974).

P. Heller, Rep. Prog. Phys. 30, 731 (1967).

P.C. Hemmer and G. Stell, Phys. Rev. Lett. 24, 1284 (1970).

P.C. Hemmer and G. Stell, J. Chem. Phys. 56, 4274 (1972).

R. Hocken, Ph.D. thesis, State University of New York at Stony Brook (1973, unpublished).

R. Hocken, M.A. Horowitz, and S.C. Greer, Phys. Rev. Lett. 37, 964 (1976).

R. Hocken and M.R. Moldover, Phys. Rev. Lett. 37, 29 (1976).

R. Hocken and G. Stell, Phys. Rev. A8, 887 (1973).

J. Huang and W.W. Webb, J. Chem. Phys. 50, 3677 (1969).

D.C. Jones and S. Amstell, J. Chem. Soc. 1930, 1316 (1930).

L.P. Kadanoff, W. Götze, D. Hamblen, R. Hecht, E.A.S. Lewis, V.V. Palciauskas, M. Rayl, J. Swift, D. Aspnes, and J. Kane, Rev. Mod. Phys. 39, 395 (1967).

L.P. Kadanoff, A. Houghton and M.C. Yalabik, J. Stat. Phys. 14, 171 (1976).

M.W. Kim and D.S. Cannell, Phys. Rev. A13, 411 (1976).

J.S. Kouvel and M.E. Fisher, Phys. Rev. 136, 1626 (1964).

D.P. Landau, Phys. Rev. B13, 2997 (1976).

S.Y. Larson, R.D. Mountain, and R. Zwanzig, J. Chem. Phys. 42, 2187 (1965).

J. Lecat, Thesis, Brussels, 1909.

T.D. Lee and C.N. Yang, Phys. Rev. 87, 410 (1952).

H.L. Lorentzen and B.B. Hansen in Misc. Publ. U.S. Nat. Bur. Stand. No. 273 ed. by M.S. Green and J.V. Sengers, p. 213 (1966).

G.B. Lubkin, Phys. Today 25, 17 (1972).

H. Lutz, J.D. Gunton, H.K. Schurmann, J.E. Crow and T. Mihalisn, Solid State Comm. 14, 1075 (1974).

K.B. Lyons, R.C. Mockler, and W.J. O'Sullivan, Phys. Rev. A10, 393 (1974).

S.K. Ma, Rev. Mod. Phys. 45, 589 (1973).

B.M. McCoy and T.T. Wu, The Two Dimensional Ising Model (Harvard U.P., Cambridge, Mass., 1973).

N.D. Mermin, Phys. Rev. Lett. 26, 169 (1971a).

N.D. Mermin, Phys. Rev. Lett. 26, 957 (1971b).

N.D. Mermin and J.J. Rehr, Phys. Rev. Lett. 26, 1155 (1971c).

L. Mistura, J. Chem. Phys. 59, 4563 (1973).

S. Miyazima, J. Phys. Soc. Japan 35, 68 (1973).

D.W. Oxtoby and H. Metiu, Phys. Rev. Lett. 36, 1092 (1976).

B.A. Scheibner, private communication, 1976.

J.M.H. Levelt Sengers in Experimental Thermodynamics of Non-Reacting Fluids (Butterworths, London, 1975), Vol. II, p. 657.

J.M.H. Levelt Sengers, W.L. Greer and J.V. Sengers, J. Phys. Chem. Ref. Data 5, 1 (1976).

M. Simon, A.A. Fannin, and C.M. Knobler, Ber. Bunsenges. Phys. Chem. 71, 3259 (1967).

R. L. Scott in Specialist Periodical Reports, Chemical Thermodynamics, ed. by M.L. McGlashen (The Chemical Society, London), Vol. II., to be published.

H.E. Stanley, Introduction to Phase Transitions and Critical Phenomena (Oxford, New York, 1971).

A. Stein and G.F. Allen, J. Phys. Chem. Ref. Data 2, 443 (1974).

J.S. Steinhart and S.R. Hart, Deep-Sea Res. 15, 497 (1968).

G. Stell and J.S. Hoye, Phys. Rev. Lett. 33, 1268 (1974).

J. Timmermans, Physico-Chemical Constants of Pure Organic Compounds (Elsevier, New York, 1965), Vol. 2, p. 158.

C. Warren and W.W. Webb, J. Chem. Phys. 50, 3694 (1969).

E.W. Washburn, editor, International Critical Tables (McGraw-Hill, New York, 1928) Vol. III, P. 397.

F.J. Wegner, Phys. Rev. B5, 4529 (1972).

J. Weiner, K.H. Langley, and N.C. Ford, Jr., Phys. Rev. Lett. 32, 879 (1974).

B. Widom and J.S. Rowlinson, J. Chem. Phys. 52, 1670 (1970).

K.G. Wilson and J. Kogut, Phys. Rept. 12C, 75 (1974).

APPENDIX

APPENDIX A

RENORMALIZATION GROUP

Some basic ideas in the Renormalization Group approach will be discussed as well as some of the methods used to calculate the critical exponents for the various models. Universality and Scaling will be shown to follow from the assumptions made in the Renormalization Group Theory. For the most part, the discussion that follows will parallel several review articles (Ma, 1973; Fisher, 1974; and Wilson and Kogut, 1974) in an effort to highlight the important results.

Imagine a d-dimensional crystal lattice of volume L^d where L is measured in units of lattice spacing. At each lattice site, x, a spin of n components is situated $\phi(x) \equiv [\phi_1(x), \ldots \phi_n(x)]$. (The number of spin components, n, determines the model and the "universality class".) If ϕ_k is the Fourier component of $\phi(x)$ then

$$\phi_i(x) = L^{-d/2} \sum_k \phi_{ik} e^{ikx}$$

where the sum over wave vectors, k, is over the L^d points in the first Brillouin zone. If H_m is the Hamiltonian--a function of all the random variables ϕ_{ik}--then the probability distribution for these random variables is $P_m \propto e^{-H_m/T}$. It is assumed that H_m is invariant under rotation in the n-dimensional spin vector space and under translation in x space. Since critical phenomena are

governed by long range interactions, which are equivalent to long wavelength fluctuations (ϕ_k with small k), then an effective Hamiltonian can be constructed that has integrated out the irrelevant random variables (the ϕ_{ik} with large k):

$$\text{(A1)} \qquad \prod_{i,k>\Lambda} \int d\phi_{ik}\, e^{-H_m/T} \equiv e^{-H(\Lambda)/T}$$

where Λ is the momentum cutoff and is much smaller than the inverse lattice spacing but still much larger than the small values of k that are of interest near the critical point. The multiple integral is taken over all ϕ_{ik}'s, i = 1, 2 . . ., n and all $k > \Lambda$. $H(\Lambda)$ provides information down to a minimum distance $1/\Lambda$ but averages out any finer details at smaller distances.

Any probability distribution, P, of these random variables, ϕ_{ik}, can be specified by a set of parameters which defines a point in a parameter space (e.g., P is represented by a point μ in this space). Then for $P \propto e^{-H}$ we can write

$$\text{(A2)} \qquad H = \sum_{m=1}^{\infty} L^{-(m-1)d} \sum_{k_1,\ldots k_{2m-1}} \sum_{i_1,\ldots i_{2m}} \phi_{i_1 k_1} \cdots \cdots \phi_{i_{2m} k_{2m}} U_{2m} + \text{const.}$$

where $k_{2m} = -(k_1 + k_2 + \ldots + k_{2m-1})$ and $U_{2m} = U_{2m}(k_1, k_2, \ldots k_{2m-1}, i_1, i_2, \ldots i_{2m})$. We assume that the system can be represented by short range interactions so that U_{2m} can be expanded in powers of k. We now have a huge parameter space with points μ giving a probability distribution: $\mu \equiv (u_2, u_4, u_6, \ldots)$ where each u_{2m} can be a function of the parameters. As will be shown shortly, only part of the parameter

space is useful. The cutoff Λ is fixed for all probability distributions or else the coupling parameters are meaningless. Also, L, which is the "block size" and tells us how many random variables there are, is not included as a parameter since we will eventually let $L \to \infty$.

Now we can consider the transformation, R_s, which takes a probablilty distribution, P, to another one, P′, which we will represent by the associated points in the parameter space: $\mu' = R_s \mu$. R_s is defined implicitly by

$$(A3) \qquad P' \propto e^{-H'} = \left[\prod_{\substack{i, \\ \Lambda/s<k'<\Lambda}} \int d\phi_{ik'} e^{-H} \right]_{\phi_{k'} \to \alpha_s \phi_{sk}}$$

where sk is the product s times k. We can extract μ' from H′ by writing H′ in the form of equation (A2) and identifying the coefficients of products of random variables. There are three steps in performing (A3); first, integrate out those $\phi_{k'}$ with k′ between Λ/s and Λ; then, relabel the random variables by enlarging the wave vectors by a factor s; and, finally, multiply all random variables by a constant factor, α_s. This reduces the number of parameters by a factor s^{-d} due to the multiple integral in (A3), or equivalently, the density of points in k space is smaller by s^{-d} by the transformation $k \to sk$ so that the volume of the system described by P′ is $L'^d = s^{-d} L^d$. We can now write H′ from (A3) in the form (A2) and using L′ and so identify μ'. The set of these transformations, R_s, where $1 \leq s \leq \infty$, is called the "renormalization group".

We have yet to consider the role of α_s, which came in the last substitution in (A3). If two successive transformations R_s and $R_{s'}$ are performed, then by (A3) they have the same result as a single transformation $R_{ss'}$ provided

(A4) $$\alpha_s \alpha_{s'} = \alpha_{ss'}.$$

Since we wish our set of transformations, R_s, to form a group we require

$$R_s R_{s'} \mu = R_{ss'} \mu$$

which in turn requires (A4). Equation (A4) requires that

$$\alpha_s = s^y$$

where y is a constant.

We can now define a point in the parameter space μ^* such that

(A5) $$R_s \mu^* = \mu^*$$

(μ^* is called a fixed point and can be found by solving this equation.) This equation is not expected to have a solution unless the y in $\alpha_s = s^y$ is properly chosen, particularly as $s \to \infty$. We would then expect a very delicate balance of powers of s in order that (A5) was satisfied. Equation (A5) can be thought of as an eigenvalue problem with eigenvectors μ^* and eigenvalues y. (Of course, R_s is not linear so we cannot say whether we shall encounter a discrete or continuous (or any at all) set of solutions.) We will assume a solution and define a new exponent, η, by $y = 1 - \eta/2$ so that $\alpha_s = s^{1-\eta/2}$. If we define the correlation function

$G(k,\mu)$ by $G(k,\mu) \equiv \langle|\phi_{ik}|^2\rangle_{p'} = \alpha_s^2 \langle|\phi_{isk}|^2\rangle_{p'} = \alpha_s^2 G(sk, R_s\mu)$, with $k < \Lambda/s$, then

(A6) $$G(k,\mu) = s^{2-\eta} G(sk, R_s\mu), \qquad k < \Lambda/s.$$

We have a way now to get from one point in the parameter space to another--by using R_s. By letting $\mu(T)$ represent our system at temperature T, then, with $T \to T_c$, we will show that $R_s\mu(T) \to \mu^*$ for large s. In particular, if T is close to T_c then we can say μ is close to μ^* so that we can expand

$$\mu - \mu^* = \delta\mu + O(\delta^2\mu)$$

and keep only the first term, i.e., <u>linearize</u> R_s. We can now use our knowledge of linear vector spaces and operators to guide us in obtaining solutions. With $\mu = \mu^* + \delta\mu$ then

$$\mu' = R_s\mu = R_s(\mu^* + \delta\mu) = \mu^* + R_s\delta\mu \equiv \mu^* + \delta\mu'$$

(A7) $$\Rightarrow \quad \delta\mu' = R_s\delta\mu.$$

R_s is a linear operator if $O(\delta^2\mu)$ terms are dropped in calculating $\delta\mu'$ from (A7). We can now use matrix techniques to solve (A7) for the eigenvectors and eigenvalues. If the eigenvalues are $\lambda_j(s)$ and the corresponding eigenvectors are e_j, $j = 1, 2, \ldots, \infty$, then we can label the eigenvalues in decreasing order: $\lambda_1 \geq \lambda_2 \geq \lambda_3 \ldots$. Since $R_s R_{s'} e_j = R_{ss'} e_j$ then

$$\lambda_j(s)\lambda_j(s') = \lambda_j(ss')$$

$$\Rightarrow \quad \lambda_j(s) = s^{y_j}$$

where y_j are constants and $y_1 \geq y_2 \geq y_3 \ldots$ since $s \geq 1$.

We can then write $\delta\mu$ as a linear combination of the eigenvectors:

$$\delta\mu = \sum_j t_j e_j$$

$$\Rightarrow \quad \delta\mu' = \sum_j t_j s^{y_j} e_j. \tag{A8}$$

Consider a model (e.g., Gaussian model) where there is only one $y_1 > 0$ with all other y_j's negative. (Most models have two y's > 0 and we will discuss this case later.) Then, if s is so large that the first term dominates, $\delta\mu' = R_s\delta\mu = t_1 s^{y_1} e_1 + O(s^{y_2})$. (We assume that $t_1 s^{y_1}$ is still small enough that the linear approximation for R_s is valid.) If $t_1 = 0$ then

$$\delta\mu' = R_s\delta\mu \to 0$$

so that μ converges to the fixed point μ^* by R_s. Wilson calls t_1 a "relevant" variable (since $y_1 > 0$) and all other t_j's "irrelevant".

We can think of the linear vector space close to μ^* being spanned by the eigenvectors e_j. The subspace with $t_1 = 0$ is the "critical surface" and points thereon will be pushed toward μ^* by R_s. Points not on the critical surface will be pushed toward e_1 but away from μ^* as shown by (A8).

To obtain the relation between the formalism we have so far and critical phenomena, we will consider R_s on the probability distribution defined in (A1), which describes fluctuations in a physical system at a definite temperature, T. We can represent this probability distribution by a point $\mu(T)$ in the parameter space. This point corresponds to a set of coupling parameters that depend smoothly on temperature. Since we have integrated out $\phi_{k'}$ for

$k' > \Lambda$ in H_m then we also expect $H(\Lambda)$ to depend smoothly on temperature. By varying T, we trace out a smooth curve in the parameter space that intersects the "critical surface" at T_c. If we are at a temperature, T, very close to T_c and if $\mu(T)$ is close to μ^* then the distance t_1 of $\mu(T)$ from the critical surface can be expanded in $T - T_c$:

$$t_1(T) = A(T - T_c) + B(T - T_c)^2 + \ldots$$

Writing

$$\mu(T) = \mu^* + \delta\mu(T)$$

or

$$R_s\delta\mu(T) = A(T - T_c)s^{1/\nu}e_1 + O(s^{y_2})$$

where $y_1 = 1/\nu$ gives (A6) to be

$$G(k,\mu(T)) = s^{2-\eta}[G(sk,\mu^* + A(T - T_c)s^{1/\nu}e_1 + O(s^{y_2}))].$$

If we let $T = T_c$ ($t_1 = 0$) and $1/k \propto s = \Lambda/2k$ (s is arbitrary) we get

$$G(k,\mu(T_c)) = k^{-2+\eta}(\Lambda/2)^{2-\eta}[G(\Lambda/2,\mu^*) + O((\Lambda/2k)^{y_2})]$$

which as $k \to 0$ goes as

$$G(k,\mu(T_c)) \propto k^{-2+\eta}, \qquad k \text{ small},$$

which defines the critical exponent η. This results since $R_s\mu(T_c) \to \mu^*$ for large $s \propto 1/k$, e.g.,

$$k/\Lambda << 2^{1/y_2}, \quad y_2 < 0.$$

The case $T - T_c > 0$, $k = 0$ can be considered by letting $s = t_1^{-\nu} \doteq [A(T - T_c)]^{-\nu}$ so that

$$G(0,\mu(T)) = t_1^{-(2-\eta)\nu}[G(0,\mu^* + e_1) + O(t^{-\nu y_2})].$$

When $(T - T_c)$ (or t_1) is small, then

$$G(0,\mu(T)) \propto (T - T_c)^{-\gamma}$$

where

(A9) $$\gamma = \nu(2 - \eta)$$

which gives a "scaling law" relating the critical exponents γ, ν and η.

Remember that $\xi = \xi_0[|T - T_c|/T_c]^{-\nu} = |t_1|^{-\nu}$ is the correlation length--the average spatial extent of the fluctuations in the critical system. This means that

$$R_s \delta\mu(T) = (s/\xi)^{1/\nu} e_1 + O(s^{y_2})$$

so that R_s decreases the correlation length by a factor s. This gives the scaling result discussed in the block construction done earlier, provided that R_s, in its linear approximation near μ^*, is dominated by one eigenvalue for large s.

The linear assumption that resulted in simple scaling does not have to be utilized. Wegner (1972) has investigated nonlinear terms and the resulting corrections to simple scaling. Such corrections have recently been found necessary to explain coexistence curve measurements in pure fluids (Estler, et.al., 1975; Hocken and Moldover, 1976). These corrections have not been found

necessary for binary mixtures unless very large temperature excursions ($\varepsilon > 10^{-2}$) are made (Greer, 1976).

We have thus provided a framework that gives us the universality of the critical exponents and the scaling relations between them. It turns out that only two critical exponents are independent (we have chosen ν and η above) and all other exponents can be written in terms of these two. For all of the resulting critical exponent relations, none have been shown, either by experiment or by direct calculation, to be invalid.

Applications

The question arises as to whether the renormalization group can provide any new predictions (scaling and universality were known long before Wilson's work). In fact, there are several, but we will only mention a few. If we use a particular model (i.e., a value for n and d) then the critical exponents can be calculated by expansions using Feynman graphs. In order to know what to expand about, we need to explain what some of the values of n and d give for the critical exponents. As it turns out, there are <u>two</u> fixed points in the parameter space--one belonging to the Gaussian model (mean field exponents) and the other to the model (value of n) used. Which fixed point is stable (and only one has been observed to be) depends on the dimensionality d of the system. For short range interactions (Ising, Heisenberg, etc., models) the magic dimensionality is $d^* = 4$. For $d \geq 4$, the Gaussian fixed point is stable and mean field values are always found for the critical exponents. Below $d = 4$, the model's fixed point is stable, so an expansion can

be done in $\varepsilon = 4 - d$ dimensions to determine the critical exponents at smaller dimensions (for ε small). Of course, $\varepsilon = 1$ and 2 ($d = 3$ and 2) are interesting cases and it is truly amazing that the exponents are as close to experimental and exact and series expansion results as they are (see Figure 28).

Another exactly soluble model (the others were the Gaussian and two-dimensional Ising) is the spherical model ($n = \infty$) which gives another starting point for expansions (in $1/n$). The d,n plane can then be "filled in" for a particular critical exponent using the approximations from Renormalization Group Theory, as shown in Figure 29. These expansions (and Figure 29) are given in Fisher's review article (Fisher, 1974) and allow one to think of a continuous spin and dimensionality space--a very useful concept when one wishes to experimentally approach a two-dimensional system.

As the dimensionality (for a fixed n) varies ($d < 4$) then the fixed point moves to a new location in the parameter space. If one then imagines going from, say, three to two dimensions, then there is a <u>crossover</u> from the bulk (three-dimensional) to the two-dimensional system as the fixed point moves to its new location. It is very difficult to determine the dimensionality directly so an alternative approach to the "crossover" from three- to two-dimensions is presented in Chapter 4.

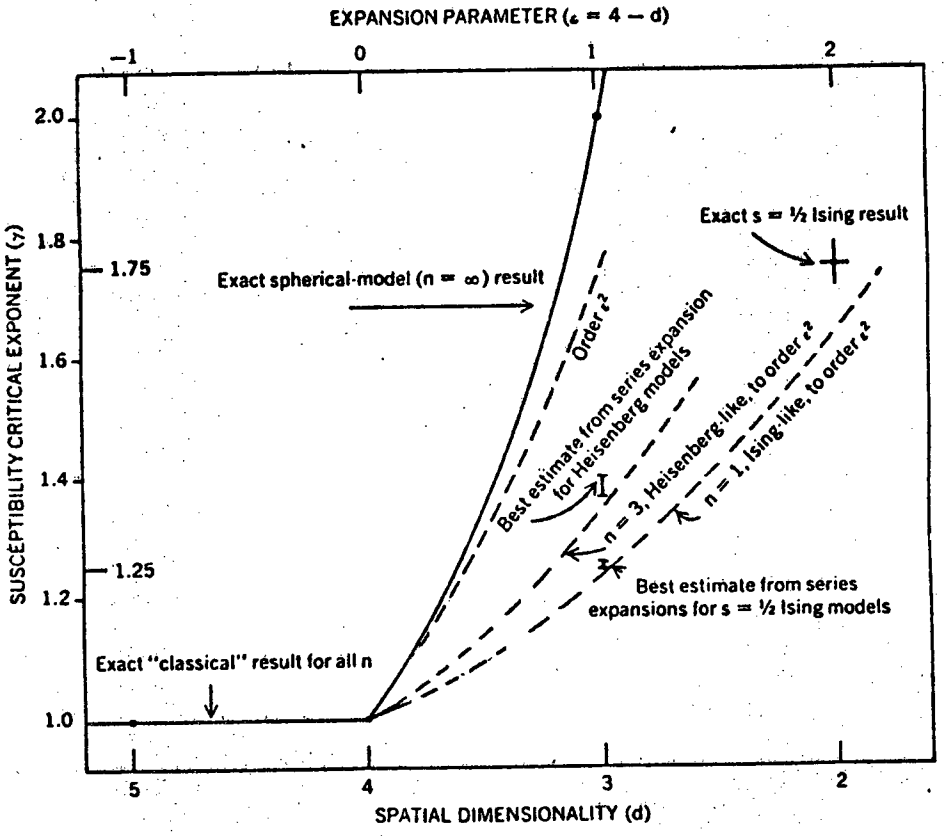

Figure 28: Predictions of the $\varepsilon = 4 - d$ expansions for the susceptibility critical exponent γ, for different spin dimensionality: $n = 1$, Ising-like (fluids, alloys, etc.); $n = 3$, Heisenberg-like (isotropic ferromagnets, etc.); $n = \infty$, which corresponds to spherical model. Dashed lines are exact second-order predictions. For $d = 2$ the exact spin-1/2 Ising-model result $\gamma = 1.75$ is indicated by cross; for $d = 3$ the best numerical estimates for Ising and Heisenberg models are shown by an I; the solid line for $n = \infty$ is the exact spherical-model result. Note that for $\varepsilon < 0$ or $d > 4$ the "classical" or mean field value $\gamma = 1$ applies for all n. (From Lubkin (1972).)

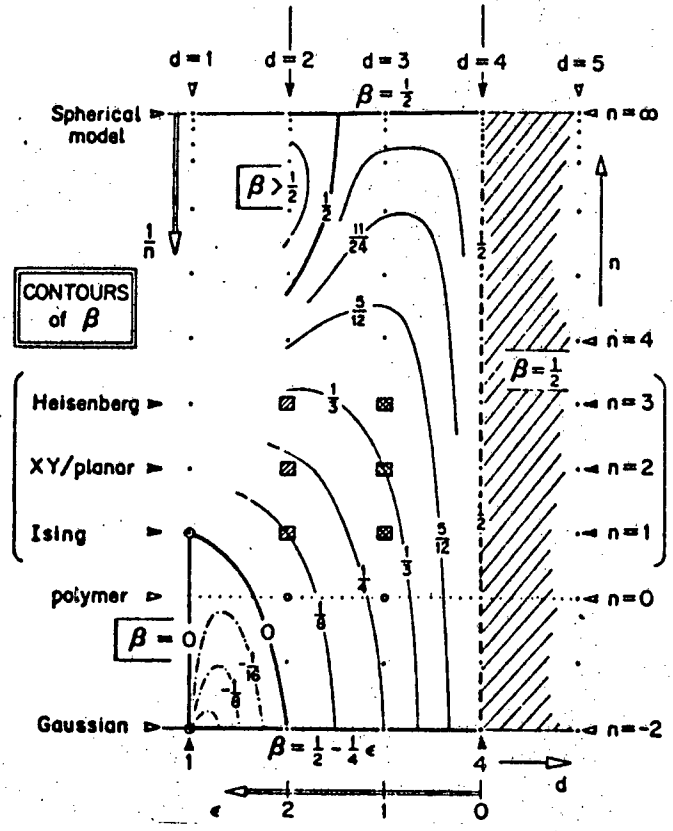

Figure 29: Diagram of the (d,n) plane showing contours of constant β as calculated from ε and 1/n expansions. There is a region where β > 1/2, and a non-physical region of negative β. (From Fisher (1974).)